Chapter 2

THE THEORY OF RADIATIVELY DRIVEN STELLAR WINDS

You must take the will for the deed.
With a heart and a half
if I could raise the wind anyhow.

James Joyce, *Ulysses*

2.1 Equations of Radiation Hydrodynamics

Stellar winds are driven by net outward forces on photospheric and circumstellar gas, and the resulting motion is determined by solving the dynamical equations of mass, momentum, and energy conservation. To apply the solutions of these partial differential equations to actual physical systems, however, it is important to understand their mathematical structure. In many cases the equations admit *time steady* wind solutions whose topology is characterized in terms of singular and critical points of the flow. In other cases no steady-state solutions exist, and the wind's velocity and density must either become non-analytic (discontinuous in value or derivatives) or time-variable. Studying various analytic and numerical methods of solving the dynamical equations can even lead to the discovery of underlying physical laws which govern the acceleration of stellar winds; e.g., we suspect, but have not yet proven, that certain time-steady wind solutions represent nonlinear "attractors" governed by new variational principles. A wealth of complex physics lies just beneath the surface of hot-star wind theory, and the present work only scratches this surface.

The first question to address, then, is that of the origin or initiation of stellar winds. We find below that both static and accelerating solutions may be possible

in some cases, but the observations clearly point to the existence of winds whenever possible. Cannon & Thomas (1977) and Andriesse (1981) propose the existence of inherent nonthermal subphotospheric instabilities that rapidly accelerate small perturbations to generate a wind, but such "sources" of mass loss are unnecessary in early-type stellar environments because of the strong force exerted by the radiation field. The maximum amount of possible mass loss is determined *in the wind* by the stellar radiation, and as much material as needed (from the near-hydrostatic atmosphere) can be "pulled up" from above. In fact, this radiation force is itself unstable to small perturbations (see Section 2.4), which may be able to amplify small deviations from a static atmosphere into a full-blown supersonic wind. Abbott (1979) and Babel (1995, 1996) investigated the limits of wind maintenance and initiation in the HR diagram, and verified that whenever radiation-driven mass loss is possible, it invariably occurs.

The idea that material can be ejected from the star by the absorption and scattering of radiation was first suggested by Milne (1924, 1926) and Johnson (1925, 1926) who found that the force on selected ions due to the absorption of photons can greatly exceed gravity. These forces, though, were assumed to be impulsive in nature, and that the accelerated ions eventually fell back down onto the star. However, Milne (1926) also predicted that these ions may be Doppler shifted out of the core of their photospheric absorption line, and thus experience a much greater force from the unattenuated continuum. Contrary to the prevailing notions, then, Milne anticipated a steady ionic outflow with an asymptotic terminal velocity v_∞ two to three times the surface escape velocity, i.e., that "the prodigal never returns."

When these theories were revived by Lucy & Solomon (1970), Castor (1974), and Castor, Abbott, & Klein (1975, hereafter CAK) in the hopes of explaining observed mass loss from O stars, the treatment was of a *single* hydrodynamic fluid driven by stellar radiation, not a heterogeneous collection of ions. This assumption of a fully-mixed, or collisionally-coupled plasma was examined by Castor et al. (1976) and justified for O-star winds. The motion of the heavy ions driven by line radiation (C, N, O, Fe, etc.) induce electrostatic forces which carry along an appropriate number of electrons, which themselves are also weakly driven by Thomson scattering. Collisions with the remaining protons and helium nuclei create a net frictional force which damps out relative motion between the various species. For winds from O and Wolf-Rayet stars, the drift velocities between these populations are found to be much smaller than the associated thermal velocities, and the one-fluid approximation is valid. For the lower-density winds around B and A stars, however, decoupling between the ions and the bulk plasma can occur and lead to "frictional heating" and high temperatures (Springmann & Pauldrach 1992; Gayley & Owocki 1994) or fully-separated multicomponent winds that may appear chemically peculiar (Babel 1995, 1996).

In this work we will assume a single-fluid treatment of a stellar wind. Starting from first principles, the hydrodynamic equations of mass, momentum, and energy conservation (Landau and Lifshitz 1987) form the basis of our wind models. For simplicity, we neglect forces due to electric and magnetic fields in these equations and defer consideration of plasma and magnetohydrodynamic effects to future work. Expressed in differential form, these equations are as follows:

$$\frac{\partial \rho}{\partial t} + \nabla \cdot (\rho \mathbf{v}) = 0 \tag{2.1}$$

$$\frac{\partial \mathbf{v}}{\partial t} + (\mathbf{v} \cdot \nabla)\mathbf{v} = -\frac{1}{\rho}\nabla P + \mathbf{g} + \frac{1}{\rho}\left[\eta \nabla^2 \mathbf{v} + (\zeta + \tfrac{1}{3}\eta)\nabla(\nabla \cdot \mathbf{v})\right] \tag{2.2}$$

$$\frac{\partial P}{\partial t} + \mathbf{v} \cdot \nabla P - \left(\frac{\gamma P}{\rho}\right)\left[\frac{\partial \rho}{\partial t} + \mathbf{v} \cdot \nabla \rho\right] = H(T) \ , \tag{2.3}$$

where the fluid velocity $\mathbf{v}$, the mass density ρ, and the gas pressure P are functions of position and time. The vector acceleration $\mathbf{g}$ includes external body forces such as gravitation and radiation forces, and the viscosity coefficients η and ζ are often considered constant. Note, however, that the low-density gas surrounding most stars is often assumed inviscid ($\eta = \zeta = 0$), and this simplification will be utilized herein (see Castor et al. 1976). Equation (2.3) represents the conservation of internal (microscopic) energy, and the constant γ is the ratio of specific heats c_P/c_V (usually 5/3 for a monatomic gas). $H(T)$ is a temperature-dependent rate of net heating or cooling.

Although the equation of energy conservation is formally required to complete the hydrodynamic system to be solved, the conditions in stellar winds often allow for an immediate, if approximate, solution to this equation. In the regions surrounding early-type stars, *radiative* heating and cooling terms in $H(T)$ dominate the energy balance, and the time scale for the gas to gain or lose energy is short when compared to the time scale of the flow. These conditions allow radiative equilibrium to be assumed throughout large parts of the wind, and a solution for the gas temperature $T(\mathbf{r})$ is thus simpler to evaluate. Klein & Castor (1978) solved the full radiative equilibrium problem for hydrogen in a spherical stellar wind, and they concluded that the electron temperature is approximately constant with radius, and slightly less than the photospheric effective temperature $T_{\rm eff}$.

This work has been extended (Stewart & Fabian 1981; Drew 1989) using more accurate statistical and thermal equilibrium calculations, and more extensive atomic data. Drew (1989) finds that the ratio of the wind temperature to the stellar $T_{\rm eff}$ shows a slow decline with radius, from $\sim$0.8 at the stellar surface to nearly $\sim$0.6 at twice the stellar radius, and is not sensitively dependent on the heavy element abundances. Bunn & Drew (1992) fit the computed temperature variation with

a function which depends only on the local wind velocity; this implies a constant asymptotic temperature as $r \to \infty$. Fortunately, the highly supersonic hydrodynamic structure of the stellar wind is relatively insensitive to these temperature variations, and we safely assume a simple isothermal $T(\mathbf{r}) = T_{\rm eff}$ in the remainder of this work.

Thus, the inviscid hydrodynamic equations of mass and momentum conservation, together with an appropriate equation of state, can be considered a closed set of five equations in five unknowns (P, ρ, $\mathbf{v}$). The spherical (or near-spherical) symmetry of stellar environments naturally leads us to express these equations in spherical polar coordinates, and in component form, as

$$\frac{\partial \rho}{\partial t} + \frac{1}{r^2}\frac{\partial}{\partial r}(\rho v_r r^2) + \frac{1}{r\sin\theta}\frac{\partial}{\partial \theta}(\rho v_\theta \sin\theta) + \frac{1}{r\sin\theta}\frac{\partial}{\partial \phi}(\rho v_\phi) = 0 \qquad (2.4)$$

$$\frac{\partial v_r}{\partial t} + v_r\frac{\partial v_r}{\partial r} + \frac{v_\theta}{r}\frac{\partial v_r}{\partial \theta} + \frac{v_\phi}{r\sin\theta}\frac{\partial v_r}{\partial \phi} - \frac{v_\theta^2 + v_\phi^2}{r} = -\frac{1}{\rho}\frac{\partial P}{\partial r} + g_r \qquad (2.5)$$

$$\frac{\partial v_\theta}{\partial t} + v_r\frac{\partial v_\theta}{\partial r} + \frac{v_\theta}{r}\frac{\partial v_\theta}{\partial \theta} + \frac{v_\phi}{r\sin\theta}\frac{\partial v_\theta}{\partial \phi} + \frac{v_r v_\theta}{r} - \frac{v_\phi^2\cot\theta}{r} = -\frac{1}{\rho r}\frac{\partial P}{\partial \theta} + g_\theta \qquad (2.6)$$

$$\frac{\partial v_\phi}{\partial t} + v_r\frac{\partial v_\phi}{\partial r} + \frac{v_\theta}{r}\frac{\partial v_\phi}{\partial \theta} + \frac{v_\phi}{r\sin\theta}\frac{\partial v_\phi}{\partial \phi} + \frac{v_r v_\phi}{r} + \frac{v_\theta v_\phi\cot\theta}{r} = -\frac{1}{\rho r\sin\theta}\frac{\partial P}{\partial \phi} + g_\phi \ . \qquad (2.7)$$

To model the wind surrounding a hot star, several additional simplifying assumptions are commonly made to facilitate solutions to the above equations. In this Chapter we examine the problem of a spherically symmetric wind (with $v_\theta = v_\phi = 0$ and all angular derivatives also zero) and explore possible time-steady configurations. Even at this simplified level, however, the equations of motion are highly nonlinear, and various methods of solution will be discussed. In subsequent Chapters we investigate multidimensional and time-dependent models of hot-star winds, which usually can only be constructed numerically.

Consider a spherical star of mass M_*, radius R_*, and bolometric luminosity L_*, with a time-steady and spherically-symmetric wind. The hydrodynamic equations reduce to one-dimensional (radial) forms. The equation of mass conservation is thus

$$\frac{1}{r^2}\frac{\partial}{\partial r}(\rho v_r r^2) = 0 \ , \qquad (2.8)$$

which can be easily integrated and formed into a constraint on the total outward *mass flux* (the amount of mass lost by the entire star per unit time),

$$\dot{M} \equiv -\frac{dM_*}{dt} = 4\pi\rho v r^2 = \text{constant} \ , \qquad (2.9)$$

replacing v_r by v in this one-dimensional analysis. This constraint will later allow us to eliminate the density ρ from the momentum equation.

The radial component of the momentum equation is given by

$$v\frac{\partial v}{\partial r} = -\frac{1}{\rho}\frac{\partial P}{\partial r} + g_r \quad . \tag{2.10}$$

To evaluate the pressure P it is useful to assume an ideal gas equation of state of the form

$$P = \frac{\rho k_B T}{\mu m_H} = \rho a^2 \quad , \tag{2.11}$$

where a is the isothermal sound speed, k_B is Boltzmann's constant, μ is the mean molecular weight of gas particles, and m_H is the mass of a hydrogen atom. The mean molecular mass in the case of complete ionization can be approximated by

$$\frac{1}{\mu} = 2X + \tfrac{3}{4}Y + \tfrac{1}{2}Z \quad , \tag{2.12}$$

where X, Y, and Z represent the mass fractions of hydrogen, helium, and heavy elements in the wind (Mihalas 1978). In all models of O and B stars in this work we assume solar-like elemental abundances ($X = 0.73$, $Y = 0.24$, $Z = 0.03$), but in models of Wolf-Rayet winds we assume a pure helium state ($Y = 1$) for simplicity.

If the gas temperature T, and thus the sound speed a, is assumed to be a known function of radius, the mass flux constraint above can be used to eliminate the density ρ, and the resulting equation of motion reduces to

$$\left(v - \frac{a^2}{v}\right)\frac{dv}{dr} = \frac{2a^2}{r} - \frac{da^2}{dr} + g_r \quad . \tag{2.13}$$

The external acceleration g_r can be written as a sum of gravitational and radiation forces, where the radiation field is naturally separable into that due to the continuum and spectral lines,

$$g_r = -\frac{GM_*}{r^2} + g_{\rm rad}^C + g_{\rm rad}^L \quad . \tag{2.14}$$

The radiative force terms are derived in their entirety in Section 2.2, but can be parameterized in some cases rather simply. In contrast to the stellar interior, where thermodynamic equilibrium allows the radiation force to be expressed as the gradient of a scalar isotropic "radiation pressure," the nonlocal character of the radiation field in the expanding circumstellar gas (and its associated dependence on the wind *velocity*) does not allow this simplification, and knowledge of the dynamic properties of the fluid is required.

2.2 The Sobolev Radiation Force

2.2.1 The Continuum and Individual Lines

Radiation is able to transfer momentum to matter via the absorption and scattering of photons. The acceleration (force per unit mass) due to a radiation field at a point $\mathbf{r}$ (Mihalas 1978) is given by

$$\mathbf{g}_{\rm rad}(\mathbf{r}) = \frac{1}{c} \oint \int_{\nu=0}^{\infty} \kappa_\nu I_\nu(\mathbf{r},\hat{\mathbf{n}})\, \hat{\mathbf{n}}\, d\Omega\, d\nu \tag{2.15}$$

$$= \frac{1}{c} \int_{\nu=0}^{\infty} \kappa_\nu \boldsymbol{\mathcal{F}}_\nu(\mathbf{r}) d\nu \quad , \tag{2.16}$$

where κ_ν is the total (absorption plus scattering) mass extinction coefficient (in $\rm cm^2/g$) which is assumed to be isotropic (i.e., independent of direction Ω). The variables I_ν and $\boldsymbol{\mathcal{F}}_\nu$ are the monochromatic radiative intensity and flux, respectively, and the unit vector $\hat{\mathbf{n}}$ is the direction of flow of the radiation, over which the intensity moment is integrated over solid angle Ω.

We can separate the opacity and radiation field into continuum (in hot stars, presumed dominated by electron scattering) and line processes. Although spectral lines subtend only narrow bands of wavelength, they play an important role in wind driving. This is because bound atoms *resonate,* or constructively interfere with continuum photons. This broad-band excitation of a resonance is the same effect that makes a whistle loud or a laser bright; the response remains significant even when averaged over the entire continuum (see Gayley 1995). Thus, treatment of both continuum and line radiation driving is important in hot-star wind theory, and the force can be separated into two general components:

$$\mathbf{g}_{\rm rad} = \mathbf{g}^C_{\rm rad} + \mathbf{g}^L_{\rm rad} \tag{2.17}$$

$$= \frac{\sigma_e}{c} \oint \int_{\nu=0}^{\infty} I_\nu(\mathbf{r},\hat{\mathbf{n}})\, \hat{\mathbf{n}}\, d\Omega\, d\nu \;+ \sum_{\rm lines} \frac{\kappa_L}{c} \oint \int_{\nu=0}^{\infty} \tilde{\phi}(\nu-\nu')\, I_\nu(\mathbf{r},\hat{\mathbf{n}})\, \hat{\mathbf{n}}\, d\Omega\, d\nu \quad , \tag{2.18}$$

where σ_e is the Thomson scattering opacity, κ_L is the mass absorption coefficient of a single line, and $\tilde{\phi}(\nu)$ is a normalized line profile function. Note that if the gas at position $\mathbf{r}$ is *in motion,* the frequency of radiation ν' seen at $\mathbf{r}$ will be Doppler shifted, to first order, by

$$\nu' = \nu_o \left[1 + \frac{1}{c} \hat{\mathbf{n}} \cdot \mathbf{v}(\mathbf{r}) \right] \quad . \tag{2.19}$$

Here, ν_o is the emitted frequency and $\mathbf{v}(\mathbf{r})$ is the flow velocity of the gas, assumed nonrelativistic. Let us make the standard change of variables, defining the dimensionless frequency displacement (from line center) in Doppler units as

$$x \equiv \left(\frac{\nu - \nu_o}{\Delta\nu_D} \right) \ , \tag{2.20}$$

where the Doppler width $\Delta\nu_D = \nu_o v_{th}/c$, and v_{th} is the ion thermal speed in the gas. This thermal velocity is a sensitive parameter in many wind models, and is defined from kinetic theory in a similar way as the isothermal sound speed a (eq. [2.11]),

$$v_{th} \ = \ \sqrt{\frac{2k_B T}{A_i m_H}} \ , \tag{2.21}$$

where A_i is the mean atomic weight of the driving ions in question. For ions of heavy elements such as carbon, nitrogen, and oxygen, the ratio v_{th}/a is of the order 0.2–0.3. However, many authors define a "fiducial" thermal speed of a gas composed primarily of hydrogen ions ($A_i = 1$), with a ratio $v_{th}/a \gtrsim 1$. We see below (Section 2.2.3) that definitions of other important wind variables depend on this choice of v_{th}, but the radiative force *itself* does not depend on v_{th}. The radiative acceleration can thus be written as

$$\begin{aligned} \mathbf{g}_{\rm rad} \ &= \ \frac{\sigma_e}{c} \oint\!\!\int_{\nu=0}^{\infty} I_\nu(\mathbf{r},\hat{\mathbf{n}})\,\hat{\mathbf{n}}\,d\Omega\,d\nu \\ &+ \ \sum_{\rm lines} \frac{\kappa_L \Delta\nu_D}{c} \oint\!\!\int_{x=-\infty}^{\infty} \phi\!\left(x - \frac{\hat{\mathbf{n}}\cdot\mathbf{v}(\mathbf{r})}{v_{th}} \right) I_\nu(\mathbf{r},\hat{\mathbf{n}})\,\hat{\mathbf{n}}\,d\Omega\,dx \ . \end{aligned} \tag{2.22}$$

Note that the line profile functions $\tilde{\phi}$ and ϕ are both normalized such that

$$\int_{\nu=0}^{\infty} \tilde{\phi}(\nu) d\nu = \int_{x=-\infty}^{\infty} \phi(x) dx = 1 \ , \tag{2.23}$$

and the lower limit of integration of the variable x is extended from $-c/v_{th}$ to $-\infty$ without appreciable error, because of the finite extent of the line's opacity in the overall spectrum. (See Section 3.1.3 for more details about the line profile function and opacity.)

Assuming the wind is optically thin to continuum radiation (as is the case in O and B stars), the continuum integral is simply the continuum bolometric flux $\boldsymbol{\mathcal{F}}_*$. The integral for the lines, however, is more complicated. Note that the general equation of radiative transfer,

$$\frac{dI_\nu}{d\tau_\nu} = -I_\nu + S_\nu \ , \tag{2.24}$$

has the formal solution (with a diffuse term and a "core" boundary term),

$$I_\nu(\tau_\nu) = \int_0^{\tau_\nu} S_\nu(t_\nu) e^{-(\tau_\nu - t_\nu)} dt_\nu \; + \; I_\nu^{\rm core} e^{-\tau_\nu} \quad , \tag{2.25}$$

where $S_\nu(\tau_\nu)$ is the source function of the medium, and the geometry-independent optical depth τ_ν is defined, in the moving medium along a general ray of path length s, as

$$\tau_\nu = \int_0^s \kappa_L \, \rho(s') \, \phi\left(x - \frac{\hat{\mathbf{n}} \cdot \mathbf{v}(\mathbf{r})}{v_{th}} \right) ds' \quad . \tag{2.26}$$

With the assumptions of isotropic scattering and local thermodynamic equilibrium (LTE), the source function is given by

$$S_\nu = \epsilon_\nu B_\nu(T) + (1 - \epsilon_\nu) J_\nu \quad , \tag{2.27}$$

where ϵ_ν is the photon destruction probability per scattering (absorption albedo), $B_\nu(T)$ is the Planck function, and J_ν is the mean intensity,

$$J_\nu = \frac{1}{4\pi} \oint I_\nu(\mathbf{r}, \hat{\mathbf{n}}) \, d\Omega \quad . \tag{2.28}$$

In the frame of reference of a moving atom, we assume the scattering can be considered coherent. But the thermal Doppler motion of the gas tends to produce a nearly complete frequency redistribution in the rest frame (Hummer 1969; Castor 1970; Hummer & Rybicki 1992), which greatly simplifies the form of the source function. Because the wind is an *expanding* medium, photons scattered into all directions will be systematically red-shifted in comoving wavelength. Thus, whether the line is dominated by absorption or scattering processes, photons will "drift" from the blue to red edge, and emerge with roughly fore-aft symmetry. The net diffuse component of the *force*, which is proportional to the integral of the now direction-independent intensity, times the "odd" factor of $\hat{\mathbf{n}}$, will be negligibly small. Castor (1974) estimates the ratio of the diffuse force to the "direct" core force, and finds it to be of the order of $(v_{th}/|\mathbf{v}|)$, which is indeed negligible in most of the wind.

Let us then keep only the direct term $I_\nu^{\rm core} e^{-\tau_\nu}$ from the formal solution for the intensity, and the radiative acceleration can be written as

$$\mathbf{g}_{\rm rad} = \frac{\sigma_e \boldsymbol{\mathcal{F}}_*}{c} + \sum_{\rm lines} \frac{\kappa_L \Delta\nu_D}{c} \oint \int_{x=-\infty}^{\infty} \phi \left(x - \frac{\hat{\mathbf{n}} \cdot \mathbf{v}(\mathbf{r})}{v_{th}} \right) I_\nu^{\rm core} e^{-\tau_\nu} \, \hat{\mathbf{n}} \, d\Omega \, dx \quad . \tag{2.29}$$

In a wind with a monotonically increasing velocity, one can simplify the optical depth integral (eq. [2.26]), by invoking the *Sobolev approximation* (Sobolev 1957, 1960), assuming that the variables κ_L and ρ do not change appreciably over a "Sobolev length" $L_{\rm Sob}$. If the fluid velocity is large enough, the Doppler shift of

the line frequency will dominate the integrand, and it will be sharply-peaked near the point at which the frequency x is in resonance with the local component of the fluid velocity. The frequency of the line, at "observer" position $\mathbf{r}$, is changed by one Doppler width $\Delta\nu_D$ over a length scale $L_{\rm Sob}$ on which the gas velocity $\mathbf{v}$ is increased by v_{th} (the local thermal speed of the scattering ions). Thus, if $L_{\rm Sob}$ is significantly smaller than a typical hydrodynamical scale height H_ρ, then the optical depth integral becomes a function of *local* variables only, and is dominated by the Doppler shift of the line profile. If

$$L_{\rm Sob} \approx \frac{v_{th}}{dv/dr} \ll H_\rho = \frac{\rho}{d\rho/dr} \approx \frac{v}{dv/dr} \quad , \tag{2.30}$$

then a necessary condition for the Sobolev approximation is either the zero thermal speed ($v_{th} \to 0$) limit, or the roughly equivalent limit of a supersonic wind ($v \gg v_{th}$). Note the fact that $v_{th} \approx 0.3a$ for the driving ions, so the Sobolev approximation is reasonably valid at the dynamically important *sonic point* of the flow, where $v = a$. The local variables κ_L and ρ can thus be taken out of the optical depth integral, and

$$\tau_\nu(\mathbf{r}) = \kappa_L\, \rho(\mathbf{r}) \int_0^s \phi\left(x - \frac{\hat{\mathbf{n}}\cdot\mathbf{v}(\mathbf{r}')}{v_{th}}\right) ds' \quad , \tag{2.31}$$

where the path length ranges from the stellar surface at $s' = 0$ (position vector $\mathbf{r}_0$) to the "observer" in the wind at $s' = s$ (position vector $\mathbf{r}$), with the instantaneous position $\mathbf{r}' = \mathbf{r}_0 + s'\hat{\mathbf{n}}$. Because of the assumed monotonic nature of the flow, we can make a one-to-one change of variables into frequency space:

$$x' = x - \frac{\hat{\mathbf{n}}\cdot\mathbf{v}(\mathbf{r}')}{v_{th}} \quad , \tag{2.32}$$

$$dx' = -\frac{1}{v_{th}} d\left[\hat{\mathbf{n}}\cdot\mathbf{v}(\mathbf{r}')\right] = -\frac{1}{v_{th}} \hat{\mathbf{n}}\cdot\nabla\left[\hat{\mathbf{n}}\cdot\mathbf{v}(\mathbf{r}')\right] ds' \quad , \tag{2.33}$$

since $d\mathbf{r}' = \hat{\mathbf{n}}\, ds'$, and $\hat{\mathbf{n}}$ is (for now) a constant vector. The velocity gradient term $\hat{\mathbf{n}}\cdot\nabla[\hat{\mathbf{n}}\cdot\mathbf{v}(\mathbf{r})]$, which emerges from the change of variables, is an important component of the Sobolev radiative acceleration. This variable is similarly "macroscopic," or slowly-varying over the spatial scale of an acceleration through v_{th}, and can be taken out of the integral with κ_L and ρ. The optical depth in the Sobolev approximation is then

$$\tau_\nu(\mathbf{r}) = \frac{\kappa_L\, v_{th}\, \rho(\mathbf{r})}{\hat{\mathbf{n}}\cdot\nabla\left[\hat{\mathbf{n}}\cdot\mathbf{v}(\mathbf{r})\right]} \int_{x - \hat{\mathbf{n}}\cdot\mathbf{v}(\mathbf{r})/v_{th}}^{\infty} \phi(x')dx' \quad , \tag{2.34}$$

with the $s' = 0$ limit replaced by $x' \to \infty$, because the photon is most probably completely out of the line's influence far from $\mathbf{r}$. One can define the "Sobolev optical depth" by grouping the slowly-varying variables taken out of the optical depth integral,

$$\tau_o \equiv \kappa_L\, \rho \left(\frac{v_{th}}{|\hat{\mathbf{n}}\cdot\nabla\left[\hat{\mathbf{n}}\cdot\mathbf{v}(\mathbf{r})\right]|}\right) = \kappa_L\, \rho\, L_{\rm Sob} \quad , \tag{2.35}$$

which also provides a more rigorous definition for $L_{\rm Sob}$. Note that the velocity gradient term, $\hat{\mathbf{n}} \cdot \nabla [\hat{\mathbf{n}} \cdot \mathbf{v}(\mathbf{r})]$, represents the projected component of the gradient of the velocity component which is projected along the ray $\hat{\mathbf{n}}$, and can be denoted schematically as $(\partial v_n / \partial n)$. The absolute value of this quantity is taken because the Sobolev approximation works in monotonically accelerating or decelerating velocity fields. We will ignore this absolute value for the remainder of this Chapter, but will re-examine its usefulness in subsequent Chapters dealing with more complex multidimensional winds. One can also define the known integral

$$\Phi(x, \mathbf{r}) \equiv \int_{x - \hat{\mathbf{n}} \cdot \mathbf{v}(\mathbf{r})/v_{th}}^{\infty} \phi(x') dx' \ , \tag{2.36}$$

which is proportional to the error function for a pure Doppler-broadened (i.e., Gaussian) profile, or is a step function for an infinitely sharp ("delta function") line profile. Thus, the line radiation force can be written as

$$\mathbf{g}^L_{\rm rad} = \sum_{\rm lines} \frac{\kappa_L \Delta \nu_D}{c} \oint \int_{x=-\infty}^{\infty} \phi(x') I^{\rm core}_{\nu} e^{-\tau_o \Phi(x, \mathbf{r})} \, \hat{\mathbf{n}} \, d\Omega \, dx \ . \tag{2.37}$$

Because of the limited extent in frequency of most spectral lines, the core intensity $I^{\rm core}_{\nu}$ can be safely assumed to be constant over the line, and taken out of the integral over the *line profile* frequency variable x. This intensity can be assumed to be a continuum quantity I^C. Thus, the integral becomes analytic, since

$$\begin{aligned} \mathbf{g}^L_{\rm rad} &= \sum_{\rm lines} \frac{\kappa_L \, \Delta \nu_D}{c} \oint d\Omega \, \hat{\mathbf{n}} \, I^C(\Omega) \int_{x=-\infty}^{\infty} e^{-\tau_o \Phi(x, \mathbf{r})} \, d\Phi(x, \mathbf{r}) \\ &= \sum_{\rm lines} \frac{\kappa_L \, \nu_o \, v_{th}}{c^2} \oint d\Omega \, \hat{\mathbf{n}} \, I^C(\Omega) \left[\frac{1 - e^{-\tau_o}}{\tau_o} \right] \ . \end{aligned} \tag{2.38}$$

This integral thus represents the general application of the Sobolev approximation to the force from a sum of spectral lines (Castor 1974).

2.2.2 Simple Force Estimates

The radiative acceleration due to resonant line photons is most rigorously computed by summing over "line lists" of thousands or millions of individual atomic transitions. In this dissertation, however, I review several simpler methods of estimating this sum which preserve the most important physics of line driving. Let us first consider the radiation force from a "point source" of radiation on a *single* line. This approximation was the original (Lucy & Solomon 1970; CAK) and intuitively simplest way to view the stellar radiation field, and is geometrically valid in the limit of the wind very far from the star. The direct stellar intensity reduces to

$$I^C(\Omega) = \left(\frac{L_{\nu}}{4 \pi r^2} \right) \delta(\hat{\mathbf{n}} - \frac{\mathbf{r}}{|\mathbf{r}|}) \ , \tag{2.39}$$

where L_ν represents the star's source luminosity spectrum, and the delta function is merely a schematic way of saying that $\hat{\mathbf{n}}$ and $\mathbf{r}$ are parallel for rays coming from the point-star at the origin. The projected velocity gradient $\hat{\mathbf{n}} \cdot \nabla(\hat{\mathbf{n}} \cdot \mathbf{v})$ is simply $\partial v_r / \partial r$ in this limit.

The continuum radiative acceleration due to Thomson scattering of electrons can be written as a scalar quantity, since the radial components of all vectors are all that survive, and is

$$g^C_{\rm rad} = \frac{\sigma_e L_*}{4\pi r^2 c} \ , \tag{2.40}$$

where the continuum bolometric flux has been assumed to be simply $L_*/4\pi r^2$. For a mixture of ionized gases, the Thomson scattering opacity can be expressed as

$$\sigma_e = \tfrac{1}{2}\sigma_H \left(\frac{2X+Y}{X+Y}\right) \approx \tfrac{1}{2}\sigma_H (1+X) \ , \tag{2.41}$$

with $\sigma_H = 8\pi e^4 / 3 m_H m_e^2 c^4 = 0.39778$ cm^2/g for pure hydrogen (Mihalas 1978). It is common to group the gravitational and continuum radiation force terms because they both vary as the inverse square of the radius, and

$$g + g^C_{\rm rad} = -\frac{GM_*(1-,)}{r^2} \ , \tag{2.42}$$

where the continuum Eddington ratio (L_*/L_{Edd}) is defined as

$$, = \frac{\sigma_e L_*}{4\pi c G M_*} \approx 1.5218 \times 10^{-5} (1+X) \frac{(L_*/L_\odot)}{(M_*/M_\odot)} \ , \tag{2.43}$$

and does not consider other continuum opacity sources (e.g., bound-free or free-free absorption) which are relatively unimportant in winds from O and early-B stars. The assumption that the wind is optically thin to continuum radiation is implicit in this development. By definition, , must be less than unity for stars which have a static "core." Stars existing above the Eddington limit of , $= 1$ have a net *outward* combined gravitational and continuum radiation force, and cannot hold themselves together in a time-steady sense. It is suspected that the strong outbursts of luminous blue variable (LBV) stars are due to a temporary breach of this Eddington limit (see Humphreys & Davidson 1994).

The force due to a single spectral line is also a purely radial scalar, and can be written

$$g^L_{\rm rad} = \frac{\kappa_L \, v_{th}}{c^2} \left(\frac{\nu_o L_\nu}{L_*}\right) \frac{L_*}{4\pi r^2} \left[\frac{1 - e^{-\tau_o}}{\tau_o}\right] \ . \tag{2.44}$$

Note that the quantity $(\nu_o L_\nu / L_*)$ depends on the product of L_ν and the line frequency ν_o itself. If we assume, however, that the line in question has a frequency

near the peak of the continuum spectrum, this ratio is of order unity and can be ignored. For optically thin lines, $\tau_o \ll 1$, the expression in square brackets approaches unity, and the force falls off as the inverse square of the radius, like gravity and the continuum radiation force. For optically thick lines, $\tau_o \gg 1$, the exponential $e^{-\tau_o}$ becomes negligible, and

$$g^L_{\rm rad} = \frac{\kappa_L\, v_{th}}{c^2}\frac{L_*}{4\pi r^2}\left(\frac{1}{\tau_o}\right) = \frac{L_*}{4\pi r^2 \rho c^2}\left(\frac{\partial v_r}{\partial r}\right) \quad . \tag{2.45}$$

The linear dependence of the force on the velocity gradient can be understood by recalling how the number of photons scattered in a line depends on the red-shift due to the expanding medium, and when optically thick, all photons in resonance with the line are scattered. The counter-intuitive notion of a force which both *causes* and *requires* an acceleration is a central feature of Sobolev wind driving, and the nonlinear "feedback" of this acceleration dependency is discussed further in Section 2.3.

One can approximately consider the effect of many lines by assuming an ensemble of $N_{\rm thick}$ optically thick lines and $N_{\rm thin}$ optically thin lines. The thin lines help to "cancel out" a fraction of the gravity and result in an effective gravitational acceleration

$$g_{\rm eff} \equiv g + g^C_{\rm rad} + g^L_{\rm rad}({\rm thin}) = -\frac{GM(1-\,,\,-\,,\,{\rm thin})}{r^2} \quad , \tag{2.46}$$

where

$$,\,{\rm thin} = \frac{N_{\rm thin}\kappa_L(v_{th}/c)L_*}{4\pi c G M_*} \tag{2.47}$$

is constant throughout the wind. (Actually, there are virtually an infinite number of weak lines in the spectrum, but the opacity contribution of each is minimal; the product $N_{\rm thin}\kappa_L$, however, can be finite and appreciable.) The resulting $g_{\rm eff}$ must be negative in the near-static photosphere so that the star can hold itself together. Thus, although thin lines can help reduce the effective gravity, only thick lines (which interact with the velocity gradient) can produce actual outward *wind driving* above the stellar surface. Chen & Marlborough (1994) propose an additional radial dependence for a force due to thin lines, and are thus able to accelerate a wind artificially with only thin lines. Non-Sobolev effects may introduce such terms for the B stars discussed by Chen & Marlborough, but the large mass loss rates they attempt to model will probably not result from these corrections (Babel 1996).

Because the thick-line radiative acceleration scales with the velocity gradient $\partial v_r/\partial r$, it can balance the *inertial* term in the radial momentum equation. If we assume these two terms balance each other, then

$$v_r\left(\frac{\partial v_r}{\partial r}\right) = N_{\rm thick}\,\frac{L_*}{4\pi r^2 \rho c^2}\left(\frac{\partial v_r}{\partial r}\right) \quad , \tag{2.48}$$

and the mass loss rate is naturally given by eq. (2.9) as

$$\dot{M} = 4\pi\rho v_r r^2 = N_{\rm thick}\,\frac{L_*}{c^2} \quad . \tag{2.49}$$

Also, the asymptotic wind momentum flux can be represented by

$$\dot{M}v_\infty = N_{\rm thick}\,\frac{L_*}{c^2}\,v_\infty = \frac{L_*}{c}(N_{\rm thick}\frac{v_\infty}{c}) \quad . \tag{2.50}$$

Note that we assume that the lines do not interact with one another (and thus sum individually), but this depends crucially on their relative spacing throughout the spectrum. This "single-scattering" limit implies that a photon, which sweeps out a Doppler velocity range of width v_∞ from the stellar surface to infinity, does not encounter any other lines. The spacing of thick lines, roughly,

$$\Delta v \approx \frac{c}{N_{\rm thick}} \quad , \tag{2.51}$$

must be greater than v_∞ for single-scattering to be valid. Of course, some line overlap always exists, but its overall effect on the force should be statistically balanced by regions of line paucity. Thus, it is often useful to consider the ratio of momentum flux due to the wind to that due to photons ("momentum efficiency")

$$\frac{\dot{M}v_\infty}{L_*/c} \approx \frac{v_\infty}{\Delta v} \quad , \tag{2.52}$$

which is often less than or equal to unity in the case of O and B star winds (where the single-scattering limit is a good approximation). However, Wolf-Rayet stars can exhibit values of this ratio as large as 5 to 50, implying densely-spaced and multiply-scattered lines (Willis 1991; Lucy & Abbott 1993; Gayley, Owocki, & Cranmer 1995). The fundamental upper limit to this ratio, assuming that finding enough lines is not a problem, comes when the *energy* efficiency (ratio of wind kinetic to photon energy) approaches unity, i.e., when

$$\frac{\frac{1}{2}\dot{M}v_\infty^2}{L_*} \;=\; \left(\frac{\dot{M}v_\infty}{L_*/c}\right)\frac{v_\infty}{2c} \;\rightarrow\; 1 \quad . \tag{2.53}$$

In this limit, the energy expended by the radiation field to accelerate the wind comes at the *expense* of a reduction in the radiative energy flux itself. This "photon tiring" may be a significant effect in the near-Eddington-limit (, ≈ 1) winds of LBV stars, but is negligible for most O, B, and Wolf-Rayet stars. The above energy ratio ranges from $\sim$ 0.1–2% for O and B stars, and can reach as high as $\sim$10% for Wolf-Rayet stars, but these values are well below the photon tiring limit.

2.2.3 General Line Ensemble Forces

Instead of a sum of thin and thick lines, the actual ensemble of driving lines exhibits a continuous range of optical depth τ_o. The significant insight of CAK was to model this as a statistical distribution function of line strengths. CAK first considered an extensive list of subordinate C^{+3} lines and parameterized their contribution via a power law fit, in terms of a scaled electron-scattering optical depth t:

$$g^L_{\rm rad} \propto kt^{-\alpha} \ , \qquad \text{where} \quad t \equiv \frac{\sigma_e \rho \, v_{th}}{\partial v_r / \partial r} \ . \tag{2.54}$$

CAK and Abbott (1980) realized that this power law could be expressed equivalently as a *number distribution* of lines, and Owocki, Castor, & Rybicki (1988, hereafter OCR) generalized this, and defined an exponentially-truncated power law number distribution of the form,

$$\frac{dN}{d\kappa_L} = \frac{1}{\kappa_o} \left(\frac{\kappa_L}{\kappa_o} \right)^{\alpha-2} e^{-\kappa_L/\kappa \rm max} \ , \quad 0 < \alpha < 1 \ , \tag{2.55}$$

and κ_o is related to CAK's force constant k by

$$\frac{\kappa_o v_{th}}{c} = \sigma_e \left(\frac{v_{th}}{c} \right)^{-\alpha/(1-\alpha)} \left[\frac{(1-\alpha)}{,(\alpha)} k \right]^{1/(1-\alpha)} \ , \tag{2.56}$$

where $,(\alpha)$ is the complete gamma function. The power-law exponent α characterizes the relative importance of optically thin and thick lines in the distribution: when $\alpha = 0$, all lines are thin, and when $\alpha = 1$, all lines are thick. Detailed line-list computations have found $\alpha \approx 0.5$–0.7 for various stellar environments (CAK; Abbott 1982a; Kudritzki, Pauldrach, & Puls 1987; Pauldrach et al. 1990; Shimada et al. 1994). Also, simple models of an "ensemble" of hydrogen-like resonance lines with Kramers-opacity transition strengths yield the analytic result $\alpha = 2/3$ (J. Puls, private communication).

The exponential "cut-off" parameter $\kappa_{\rm max}$ was introduced by OCR because a pure power law cannot model the fact that there must exist a single strongest optically thick line. The overall effect of $\kappa_{\rm max}$ is thus to limit the effect of strong driving lines. Theoretically, the value of $\kappa_{\rm max}$ should be equal to (or at least of the same order as) κ_o, in order to position the exponential cut-off near the point where $N(\kappa_L) = 1$, and thus avoid modeling fractions of lines. Note that the line-list distribution $dN/d\kappa_L$ assumes no overlap in the influence of the lines, and thus uses the single-scattering limit discussed above. In addition, the distribution has been "flux-weighted" in frequency such that

$$\frac{dN}{d\kappa_L} = \int_0^\infty d\nu \left(\frac{\nu L_\nu}{L_*} \right) \frac{dN_\nu}{d\kappa_L} \ , \tag{2.57}$$

and lines near the peak of the continuum spectrum have a stronger contribution to the distribution.

The sum over lines in the force is then replaced by an integral,

$$\sum_{\rm lines} \mathbf{g}^L_{\rm rad} = \int_0^\infty \mathbf{g}^L_{\rm rad} \frac{dN}{d\kappa_L} d\kappa_L \ , \tag{2.58}$$

and the *total* line force becomes

$$\begin{aligned}
\mathbf{g}^L_{\rm rad} &= \frac{v_{th}}{c^2} \oint d\Omega\, \hat{\mathbf{n}}\, I^C(\Omega) \int_0^\infty \kappa_L \frac{dN}{d\kappa_L} \left[\frac{1-\exp(-\kappa_L \rho L_{\rm Sob})}{\kappa_L \rho L_{\rm Sob}}\right] d\kappa_L \\
&= \frac{v_{th}}{c^2 \kappa_o^{\alpha-1}} \oint d\Omega\, \hat{\mathbf{n}}\, I^C(\Omega) \int_0^\infty \left(\frac{\kappa_L^{\alpha-1}}{e^{\kappa_L/\kappa \rm max}}\right) \left[\frac{1-\exp(-\kappa_L \rho L_{\rm Sob})}{\kappa_L \rho L_{\rm Sob}}\right] d\kappa_L \\
&= \frac{v_{th}}{c^2 \kappa_o^{\alpha-1}} \oint d\Omega\, \hat{\mathbf{n}}\, I^C(\Omega) (\rho L_{\rm Sob})^{-\alpha} \left[\tau_{\rm max}^{\alpha-1} - \left(\frac{\tau_{\rm max}}{\tau_{\rm max}+1}\right)^{\alpha-1}\right] \frac{,(\alpha)}{\alpha-1} \ ,
\end{aligned}$$

where $\tau_{\rm max} = (\kappa_{\rm max}\, \rho\, L_{\rm Sob})$. Thus, if we follow the pure CAK power law ensemble, with $\kappa_{\rm max} \to \infty$, the first term in the square brackets will be negligibly small, and the second term will approach unity. Then,

$$\mathbf{g}^L_{\rm rad} = \frac{v_{th}}{c^2 \kappa_o^{\alpha-1}} \oint I^C(\Omega) \frac{,(\alpha)}{1-\alpha} \left[\frac{\hat{\mathbf{n}} \cdot \nabla(\hat{\mathbf{n}} \cdot \mathbf{v})}{\rho(\mathbf{r}) v_{th}}\right]^\alpha \hat{\mathbf{n}}\, d\Omega \ . \tag{2.59}$$

Now that the complete Sobolev line force has been derived for a generalized geometry, let us perform the angle integral for certain specific cases. For a radial *point source* of radiation at the origin, the core intensity is given above in eq. (2.39), and the angle integral collapses into the purely radial form,

$$\begin{aligned}
g^L_{\rm rad} &= \frac{v_{th}}{c^2 \kappa_o^{\alpha-1}} \frac{L_*}{4\pi r^2} \frac{,(\alpha)}{(1-\alpha)[\rho(r) v_{th}]^\alpha} \left(\frac{\partial v_r}{\partial r}\right)^\alpha & (2.60) \\
&= \frac{\sigma_e^{1-\alpha} L_*}{4\pi c r^2} \frac{k}{[\rho(r) v_{th}]^\alpha} \left(\frac{\partial v_r}{\partial r}\right)^\alpha \ , & (2.61)
\end{aligned}$$

using CAK's force constant k, defined in eq. (2.56). Note that k is sensitively dependent on v_{th}, and most published computations of k and α assume a fiducial hydrogen thermal velocity so that k can be defined independently of the exact composition and abundance of heavy (line driving) ions. Gayley (1995) recasts the CAK line ensemble into a form which clearly separates v_{th} and α from the normalization constant (k or κ_o), but we retain the original CAK notation here because it has become the standard convention.

Also note that the optically thin and thick limits of $\alpha = 0$ and $\alpha = 1$ are apparent in the above line acceleration, and intermediate values of α span this range continuously. This expression can be combined with the approximate thick-line expressions (2.45) and (2.51) to estimate the mean separation between thick lines in the chosen (k, α) distribution,

$$\Delta v \approx \frac{v_{th}^{\alpha}}{k} \left[\frac{1}{\sigma_e \rho} \left(\frac{\partial v_r}{\partial r} \right) \right]^{1-\alpha} \quad , \tag{2.62}$$

and the rough validity of the single-scattering limit can be directly assessed from a given model wind.

2.2.4 The Finite Stellar Disk

For a *spherical star* of finite radius R_*, the wind at a radius r will "see" a finite circular disk of radiation at the origin. Although the continuum force in the radial direction $g_{\rm rad}^C$ will be identical to the corresponding point-source force (due to Gauss' Law for the radiative flux), the line radiation term will be modified by the presence of nonradial rays from the stellar disk. Symmetry allows us to place our observer along the z-axis, and

$$\mathbf{g}_{\rm rad}^L = \frac{\sigma_e^{1-\alpha} k}{c} \oint I^C(\theta', \phi') \left[\frac{\hat{\mathbf{n}} \cdot \nabla(\hat{\mathbf{n}} \cdot \mathbf{v})}{\rho(\mathbf{r}) v_{th}} \right]^{\alpha} \hat{\mathbf{n}} \, \sin\theta' \, d\theta' \, d\phi' \quad , \tag{2.63}$$

where θ' and ϕ' are measured from the observer's position, not the origin. The azimuthal (ϕ') integral can be performed immediately, but the polar integral is less trivial.

Defining $\mu' = \cos\theta'$ and assuming a purely radial velocity field, the velocity gradient can be derived in general (Castor 1974; Koninx 1992), and is given by

$$\hat{\mathbf{n}} \cdot \nabla(\hat{\mathbf{n}} \cdot \mathbf{v}) = \mu'^2 \frac{\partial v_r}{\partial r} + (1 - \mu'^2) \frac{v_r}{r} \quad . \tag{2.64}$$

The bolometric core intensity can be written as

$$I^C(r, \theta', \phi') \; = \; \frac{L_*}{4\pi R_*^2} \, D(\mu', r) \tag{2.65}$$

where $D(\mu', r)$ is a limb darkening function. Often, a uniformly-bright disk is assumed, with

$$D(\mu', r) = \begin{cases} 0, & -1 \le \mu' < \mu_* \\ 1/\pi, & \mu_* < \mu' < +1 \end{cases} \tag{2.66}$$

where

$$\mu_*(r) \equiv \sqrt{1 - \frac{R_*^2}{r^2}} \tag{2.67}$$

defines the stellar limb, and $D(\mu', r)$ is normalized to give the same angle-integrated flux as in the point-star case, via

$$\frac{L_*}{4\pi r^2} = \frac{L_*}{4\pi R_*^2} 2\pi \int_{\mu_*}^{1} D(\mu', r)\, \mu'\, d\mu' \ . \tag{2.68}$$

Note that one could also use simple linear (grey atmosphere) limb darkening, obtained from the Eddington approximation,

$$D(\mu', r) = \begin{cases} 0, & -1 \le \mu' < \mu_* \\ (2 + 3\mu'')/4\pi, & \mu_* < \mu' < +1 \end{cases} \ , \tag{2.69}$$

where $\mu'' = \cos\theta''$, the angle on the star between radius $\mathbf{r}$ and the direction $\hat{\mathbf{n}}$ towards the point in the wind. Plane trigonometry gives this angle in terms of the observer-centered angle μ':

$$\mu'' = \sqrt{1 - \frac{r^2}{R_*^2}(1 - \mu'^2)} = \sqrt{\frac{\mu'^2 - \mu_*^2}{1 - \mu_*^2}} \ , \tag{2.70}$$

and, for completeness, the star-centered angle $\theta_o = \theta'' - \theta'$ is given by

$$\mu_o = \cos\theta_o = \frac{r}{R_*}\left[1 + \mu'\sqrt{\mu'^2 - \mu_*^2} - \mu'^2\right] \ . \tag{2.71}$$

The general radial line radiation force is now given by

$$g^L_{\rm rad} = \frac{2\pi\sigma_e^{1-\alpha}k}{c[\rho(r)v_{th}]^\alpha}\left(\frac{L_*}{4\pi R_*^2}\right)\int_{-1}^{+1} D(\mu', r)\left[\mu'^2\frac{\partial v_r}{\partial r} + (1 - \mu'^2)\frac{v_r}{r}\right]^\alpha \mu'\, d\mu' \ . \tag{2.72}$$

It is common to define and work with a *finite disk factor,* which isolates the finite disk correction to the simple point source model, and is the ratio of respective line accelerations,

$$\boldsymbol{\eta}^{\rm L} \equiv \frac{\mathbf{g}^L_{\rm rad}(\text{finite disk})}{g^L_{\rm rad}(\text{point source})} \tag{2.73}$$

$$= \frac{2\pi}{(1 - \mu_*^2)(dv_r/dr)^\alpha}\int_{-1}^{+1} D(\mu', r)\left[\mu'^2\frac{\partial v_r}{\partial r} + (1 - \mu'^2)\frac{v_r}{r}\right]^\alpha \mu'\, d\mu' \ , \tag{2.74}$$

and is, in general, a vector quantity. The finite disk factor does not depend on the wind density $\rho(\mathbf{r})$ or on the line distribution constant k, but does depend sensitively

on the exponent α. A continuum finite disk factor $\boldsymbol{\eta}^{\rm C}$ can also be defined, but for a spherical star it is purely radial with a magnitude of unity. Note that, if one defines the logarithmic derivative variable (Castor 1970)

$$\sigma = \frac{\partial \ln v_r}{\partial \ln r} - 1 = \frac{r}{v_r}\frac{\partial v_r}{\partial r} - 1 \quad , \tag{2.75}$$

then one can express the projected velocity gradient as

$$\mu'^2 \frac{\partial v_r}{\partial r} + (1-\mu'^2)\frac{v_r}{r} = \left(\frac{1+\sigma\mu'^2}{1+\sigma}\right)\frac{\partial v_r}{\partial r} \quad , \tag{2.76}$$

and the μ'-integral becomes easier to evaluate. This σ variable is a convenient measure of the anisotropy of the local velocity gradient. Very close to the star $\sigma \gg 1$, which implies the radial velocity derivative $\partial v_r/\partial r$ dominates the overall expansion. At an intermediate radius in the wind, σ drops to zero, and the expansion is locally isotropic. In the outer wind, σ asymptotically approaches -1 at large radii, and the spherical geometry, in the term v_r/r, dominates the (now mainly lateral) expansion.

For the uniformly bright disk (Castor 1974; CAK), the μ'-integral can be evaluated analytically using eq. (2.76) for the projected velocity gradient, and the radial component of the finite disk factor is

$$\eta_r^L(\text{uniform}) \equiv \eta_{un} = \frac{2}{(1-\mu_*^2)(1+\sigma)^\alpha}\int_{\mu_*}^1 (1+\sigma\mu'^2)^\alpha \mu'\, d\mu' \tag{2.77}$$

$$= \frac{(1+\sigma)^{1+\alpha} - (1+\sigma\mu_*^2)^{1+\alpha}}{\sigma(1+\alpha)(1+\sigma)^\alpha(1-\mu_*^2)} \quad . \tag{2.78}$$

Kudritzki et al. (1989) and Koninx (1992) define a convenient variable

$$\chi \equiv \frac{R_*^2}{r^2}\left[1 - \frac{v_r}{r(\partial v_r/\partial r)}\right] = (1-\mu_*^2)\left(\frac{\sigma}{\sigma+1}\right) \tag{2.79}$$

and the uniformly bright finite disk factor can be written as a function of this single variable,

$$\eta_{un} = \frac{1-(1-\chi)^{1+\alpha}}{\chi(1+\alpha)} \quad . \tag{2.80}$$

For points extremely far from the star, $r \to \infty$, $\mu_* \to 1$, and $\sigma \to -1$, η_{un} naturally approaches unity, because the star more and more resembles a true "point source." Very close to the stellar surface, however, $\mu_* \to 0$ and $\sigma \gg 1$, and in this limit, $\chi \to 1$, and

$$\eta_{un} \to \frac{1}{1+\alpha} \quad . \tag{2.81}$$

For the linearly limb-darkened disk, the finite disk factor takes the form

$$\eta_{limb} \;=\; \frac{\eta_{un}}{2} + \frac{3}{2(1-\mu_*^2)(1+\sigma)^\alpha}\int_{\mu_*}^{1}(1+\sigma\mu'^2)^\alpha\sqrt{\frac{\mu'^2-\mu_*^2}{1-\mu_*^2}}\mu'\,d\mu' \quad . \tag{2.82}$$

This integral is, in general, analytically intractable. However, for points extremely far from the star, and for the $\sigma = 0$ point, η_{limb} naturally approaches the uniformly bright η_{un} (which is unity at these radii). Very close to the star, when $\mu_* \rightarrow 0$ and $\sigma \gg 1$,

$$\frac{\eta_{limb}}{\eta_{un}} \;\rightarrow\; \frac{1}{2} + \frac{3}{2}\left(\frac{1+\alpha}{3+2\alpha}\right) \quad , \tag{2.83}$$

which only ranges between 1 and 1.1 for all allowed values of the exponent α. For example, when $\alpha = 0.5$, this ratio approaches 1.0625, and when $\alpha = 0.7$, it approaches $\sim$1.0795. Note also that for $\alpha = 0.5$, the above integral can be computed analytically, but the expression is extremely complex, and there is little practical use in transcribing this solution here. Figure 2.1 illustrates the radial dependence of η_{un} (dashed line, computed analytically) and η_{limb} (solid line, computed numerically) for various values of the exponent α, and for various velocity laws characterized by the simple fitting formula

$$v_r(r) \;=\; v_\infty\left(1-\frac{R_*}{r}\right)^\beta \quad . \tag{2.84}$$

Note that the error in assuming a uniformly bright disk is small, only 5–8% near the surface, and much less so further out.

We can assess the dynamical impact of this modified finite disk factor on a one-dimensional spherically symmetric wind by examining the equation of motion of the wind in the highly supersonic, or zero sound speed limit (Kudritzki et al. 1989; Gayley, Owocki, & Cranmer 1995). Near the surface of the star ($\sigma \gg 1$), where the mass loss rate is thought to be determined, the overall effect of any finite disk factor η on the mass loss rate $\dot{M}$ can be approximated by

$$\dot{M} \;\approx\; \eta^{1/\alpha}\,\dot{M}(\text{point source}) \quad , \tag{2.85}$$

where η is evaluated at the dynamical critical point (see Section 2.3.2 below). Thus, if we can assume the surface values of η_{limb}/η_{un} at the critical point, the effect of including limb darkening could result in a relative mass loss increase of $\sim$11% ($\alpha = 0.7$) to $\sim$13% ($\alpha = 0.5$) over the uniformly-bright models.

2.2.5 The Effect of the Ionization Balance

Abbott (1982a) performed an extensive calculation of the radiative line force using a list of bound-bound transitions spanning six stages of ionization and the

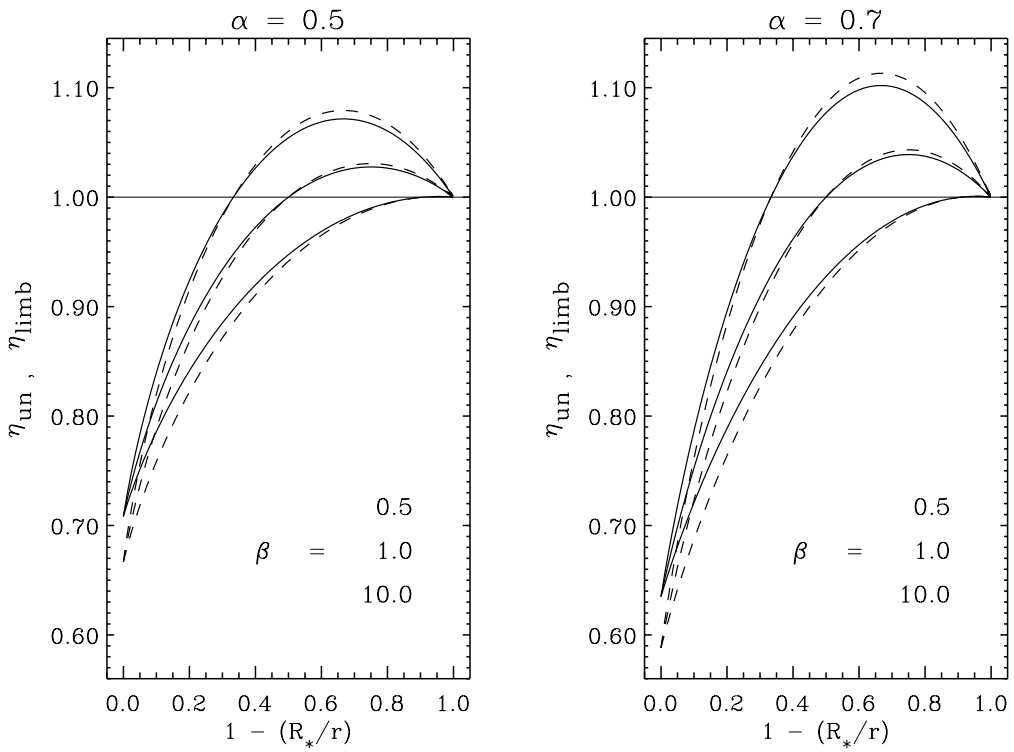

Figure 2.1: The spherical-star finite disk (FD) factor, plotted versus radius in the wind, for various models and assumptions. The dashed lines are the analytic uniformly-bright FD factors, and the solid lines are the numerically-computed FD factors with linear limb darkening. The two plots represent winds with $\alpha = 0.5$ (left) and $\alpha = 0.7$ (right), and the three sets of curves on each plot represent (from top to bottom) velocity laws with $\beta = 0.5$, 1.0, and 10.0.

elements H to Zn. This work confirmed earlier results concerning the dependence of the force on the temperature distribution and chemical composition (through, e.g., the continuum opacity σ_e), but introduced a new dependence on the relative state of ionization of the wind. It was found that, since lower ionization stages contain more lines, the force tends to increase with increasing electron number density n_e, as roughly predicted by the LTE Saha rate equation. However, because the ionization balance remains roughly constant throughout the wind, the force is relatively insensitive to this phenomenon, and is a minor (but necessary) effect. Abbott (1982a) thus assumed a weak power-law dependence on the quantity

$$N_{11} \equiv \frac{n_e}{W} \times 10^{-11}\ \mathrm{cm}^3 \ , \tag{2.86}$$

where the dimensionless "dilution factor" W is defined as the fraction of solid angle Ω_* occupied by the star for an observer at distance r, and for a spherical star,

$$W = \frac{\Omega_*}{4\pi} = \frac{1}{4\pi}\int_{\phi'=0}^{2\pi}\int_{\mu'=\mu_*}^{1} d\mu' d\phi' = \frac{1}{2}(1-\mu_*) \ , \tag{2.87}$$

and it is required to take into account the spherical geometry of the extended envelope around the star. The local radiation density is diluted by this amount as one moves away from the star, and thus affects the photoionization-recombination balance directly. Mihalas (1978, eq. [5-46]) showed that the ionization balance of spherically symmetric winds, via the population ratio (N_j/N_{j+1}), depends linearly on the above factor of (n_e/W).

For a fully-ionized gas, one can write $n_e \approx \rho/\mu m_H$, with the mean molecular weight μ defined as above in eq. (2.12), and the modified fit to the radiation line force can be written

$$g^L_{\mathrm{rad}} \ = \ \frac{GM,}{r^2} k\eta \left(\frac{1}{\sigma_e \rho v_{th}}\frac{\partial v_r}{\partial r}\right)^{\alpha} N_{11}^{\delta} \ . \tag{2.88}$$

The exponent δ typically ranges from 0.02–0.2 in early type stellar winds, and the radiative force thus depends on the density as $\rho^{\delta-\alpha}$. Pauldrach et al. (1990) more recently computed non-LTE models for the line force, using more than 10^5 transitions, and found agreement with Abbott's values of δ at $T_{\mathrm{eff}} > 35,000$ K, but found slightly lower values for cooler temperatures.

2.3 Wind Solutions

2.3.1 Nonlinear Solution Methods

The radiative acceleration derived in Section 2.2 can now be inserted into the radial momentum conservation equation derived in Section 2.1, and this equation

can be solved for the velocity law $v_r(r)$ and mass loss rate $\dot{M}$ of the wind. We proceed in this Section from approximate analytic solutions to successively more sophisticated numerical solutions, and we apply these results to a standard model of the O4f supergiant ζ Puppis (HD 66811) to compare with observations. For this model, we take $M_* = 60 M_\odot$, $R_* = 19 R_\odot$, $L_* = 8 \times 10^5 L_\odot$, and $T_{\rm eff} = 42{,}000\,{\rm K}$ (see, e.g., Howarth & Prinja 1989; Kudritzki et al. 1992). We assume an isothermal wind of temperature $T_{\rm eff}$, corresponding to a sound speed $a = 24\,{\rm km\ s^{-1}}$, and use the line-driving constants $\alpha = 0.60$, $k = 0.15$, and $\delta = 0$. The observed terminal velocity of ζ Puppis is approximately 2200–2500 km s^{-1}, and the mass loss rate, depending on the method of measurement, ranges from 2×10^{-6} to $6 \times 10^{-6}\ M_\odot {\rm yr}^{-1}$ (Prinja et al. 1990; Lamers & Leitherer 1993; Puls et al. 1996).

Using the mass flux constraint (eq. [2.9]) to eliminate the density in the line acceleration, the "CAK equation of motion" can be written in terms of the radius r, radial velocity v, and mass loss rate $\dot{M}$, as

$$\left(v - \frac{a^2}{v}\right)\frac{dv}{dr} + \frac{GM_*(1-\ ,\ )}{r^2} - \frac{2a^2}{r} + \frac{da^2}{dr} - \frac{GM_*,}{r^2} k\eta \left[\frac{4\pi}{\sigma_e v_{th} \dot{M}}\right]^\alpha \left(r^2 v \frac{dv}{dr}\right)^\alpha \ = \ 0 \ , \tag{2.89}$$

where we temporarily neglect the Abbott (1982a) δ-factor. We implement a convenient choice of dimensionless variables,

$$x \equiv \frac{r}{R_*} \quad , \quad u \equiv \frac{v}{a} \quad , \quad w \equiv \frac{r^2 v}{GM_*}\left(\frac{dv}{dr}\right) = \frac{x^2 u}{\Pi}\left(\frac{du}{dx}\right) \quad , \tag{2.90}$$

although for non-isothermal winds, the normalizing value of a must be chosen at a representative radius. Also, the CAK equation is multiplied by an overall factor of r^2/GM_* to scale out the gravitational acceleration. Note that the constant $\Pi \equiv GM_*/a^2 R_*$ is defined as the ratio of the stellar radius R_* to the density scale height $H_\rho = a^2/(GM_*/R_*^2)$ at the stellar surface. Also, Π is the ratio of twice the "Parker radius" $(GM_*/2a^2)$ to the stellar radius R_*, and is a useful constant when working with the dimensionless variables x, u, and w. The left-hand side of the equation of motion, then, is an explicit function F_1 of x, u, and w:

$$F_1(x,u,w) = \left(1 - \frac{1}{u^2}\right) w - H(x) - C\eta w^\alpha = 0 \ , \tag{2.91}$$

where

$$H(x) \ = \ , \ -1 + \frac{2x}{\Pi} + \frac{x^2}{\Pi a^2}\frac{da^2}{dx} \ , \tag{2.92}$$

$$C \ = \ , \ k\left(\frac{4\pi G M_*}{\sigma_e v_{th} \dot{M}}\right)^\alpha \ , \tag{2.93}$$

The equation $F_1 = 0$ thus needs to be solved for u and w as functions of x, the normalized radius, and for the constant $\dot{M}$, which we shall see acts as an eigenvalue of the problem.

It is becoming evident that steady-state solutions to CAK-type equations (see, e.g., Poe, Owocki, & Castor 1990) represent a kind of "attractor," where the mass loss rate $\dot{M}$ is maximized for a given set of initial parameters. However, if $\dot{M}$ is too large, and too much mass is pushed outwards, the radiative force cannot drive the material to infinity, and it falls back down on the star in a time-dependent, usually oscillatory, manner. Thus, steady-state solutions tend to exhibit a unique value of $\dot{M}$, which represents the maximum mass that can be driven to infinity, and thus is the focal point of the attractor.

The wind equation $F_1(x, u, w) = 0$ is a highly non-linear differential equation. The variable w, however, is proportional to du/dx, and if it were possible to solve for w, one could integrate the equation to find the desired velocity law $u(x)$ of the wind. Because there are different regions in the x-u phase space where there are zero, one, or two real solutions for w, one must further specify the *singularity condition*

$$F_2(x, u, w) = \frac{\partial F_1}{\partial w} = 0 \ . \tag{2.94}$$

The solution to the two equations $F_1 = 0$, $F_2 = 0$ forms a curve, the "singular locus," in phase space, which divides a region of no solutions from a region of two solutions (see Cassinelli 1979; Bjorkman 1995). Because the first class of velocity solutions $u(x)$ we wish to consider are the most well-behaved, mathematically (i.e., continuously differentiable functions of x that range from $x = 1$ to $x \to \infty$), we require that these solutions not cross this problematic singular locus.

If the wind equation were *linear* in w or du/dx, i.e., if

$$F_1^* \ = \ A_1(x, u) + \frac{du}{dx} B_1(x, u) \ = \ 0 \ , \tag{2.95}$$

then the singularity condition would demand both $A_1 = 0$ and $B_1 = 0$, and this defines a discrete set of "critical points" $\{x_c, u_c\}$ of the flow. Parker's (1958, 1963) isothermal solar wind solutions have this topology, and the only solutions which satisfy all physical boundary conditions must pass through a transsonic critical point $u_c = 1$. The velocity derivative at the critical point is given by L'Hôpital's rule,

$$\left(\frac{du}{dx}\right)_{\rm crit} \ = \ -\frac{dA_1/dx}{dB_1/dx} \ , \tag{2.96}$$

and Abbott (1980) and Koninx (1992) demonstrate that critical points are also locations where small perturbations in the flow have zero characteristic velocity in

the inertial frame of the star. Of course, solutions which do not pass through critical points are possible (e.g., Chamberlain's [1961] "breeze" solutions), but they can have drastically different boundary properties from those which do pass through critical points.

The general nonlinear form of $F_1(x,u,w)$ in the present hot-star wind analysis has a similar general character to the linear limit above in that there are critical points of the flow, existing on singular loci, which can be located using the above singularity condition and a nonlinear generalization of L'Hôpital's rule, the so-called *regularity condition,*

$$F_3(x,u,w) \equiv \frac{\partial F_1}{\partial x} + \frac{du}{dx}\frac{\partial F_1}{\partial u} \tag{2.97}$$

$$= \frac{\partial F_1}{\partial x} + \left(\frac{\Pi w}{u x^2}\right)\frac{\partial F_1}{\partial u} = 0 \ . \tag{2.98}$$

Non-critical points that lie on singular loci do not connect to analytic (continuously differentiable) solutions, so if a desired steady-state solution must "graze" a singular locus, it must do so at a critical point. Poe, Owocki, & Castor (1990) found that, in the Sobolev approach, the wind solution which carries the maximum mass loss rate to infinity is precisely that which grazes the singular locus at a critical point. (See also Bjorkman 1995 for a discussion of other formal critical points of the CAK equations.)

The three equations, $F_1 = F_2 = F_3 = 0$, almost serve to specify the critical values of x_c, u_c, and w_c, but what thwarts a straightforward solution is the fact that the value of the constant mass loss rate $\dot{M}$ (or equivalently, the constant C in eq. [2.91]) is initially unknown. Thus we have three equations and four unknowns. This problem is solved in practice by guessing a value for the critical radius x_c, and solving the system of equations for u_c, w_c, and C. With this trial critical solution in place, one needs to evaluate whether the velocity law $u(x)$ which passes through it is consistent with the assumed static stellar model. After integrating $u(x)$ from x_c down to the star's surface ($x = 1$), various tests can be performed to evaluate the consistency of the model wind. This "matching" of the core/halo boundary conditions is, in effect, the fourth piece of information required to determine all the variables at the critical point. CAK defined the stellar photosphere as the surface at which the optical depth is unity, and a continuum Sobolev optical depth variable t can be evaluated as a check:

$$t \equiv \frac{\sigma_e \rho v_{th}}{dv/dr} = \left(\frac{\sigma_e v_{th}}{4\pi G M_*}\right)\frac{\dot{M}}{w} \ , \tag{2.99}$$

where w is evaluated at $x = 1$. Note that, although t is not the true optical depth as seen by an observer at infinity, it approaches the true continuum optical depth,

$$\tau_c = \int_{R_*}^{\infty} \sigma_e \rho \, dr \;\approx\; \sigma_e \rho H_\rho \;\approx\; \sigma_e \rho \, \frac{v}{dv/dr} \;\; , \tag{2.100}$$

where H_ρ is the density scale height (related to the flow velocity scale height by the mass continuity equation), when $v \approx v_{th}$ as is the case very near the stellar surface. Near the photosphere, the wind velocity grows exceedingly small, and one can begin to assume *hydrostatic* conditions. If the near-isothermality of the gas is maintained, then the density rises (and the velocity falls) exponentially with depth, and differences of a few scale heights do not appreciably affect the overall position of the actual stellar radius (the $x = 1$ point).

Although this implies that the condition $t \approx 1$ can be used to locate the photosphere, and thus utilized to iterate to find the correct value of x_c, the use of the Thomson scattering opacity in t is suspect both in B stars, where bound-free and free-free continuum processes become important, and in Wolf-Rayet stars, where the continuum is optically thick in large regions of the wind. Thus, in practice, the most robust way to "locate the static photosphere" is to integrate downwards from the assumed x_c and evaluate the *velocity* $v(1)$ at $x = 1$ (usually via extrapolation from a numerical grid). The near-hydrostatic region is entered when $v(1) \ll a$, or $u(1) \ll 1$, and a useful condition to define the photosphere is to set a constant fraction of the sound speed, say $u(1) \approx 0.01$. Usually, if the extrapolated value of $u(1)$ is too large, then x_c is too close to the stellar surface, and if the extrapolated $u(1)$ is too small, then x_c is too large. Often, for x_c much too large, the integration may suggest a value of $u(1)$ which is unphysically negative, or there may not be solutions to the wind equation below a certain radius.

Usually, one avoids integrating outward from the critical point until the iteration process outlined above converges on the correct critical point x_c. CAK suggest a further iteration to find the temperature structure, and Pauldrach, Puls, & Kudritzki (1986, hereafter PPK) perform this using non-LTE radiative transfer, but since the wind velocity structure is quite insensitive to the temperature law, we shall consider the imposed $T(r) = T_{\rm eff}$ as correct. Lucy & Abbott (1993), however, derive a clever approximate method for determining $T(r)$ in Wolf-Rayet winds which is worthy of note. One can write the radiative force due the combined effect of continuum and lines in terms of a general "effective" scattering coefficient,

$$(g^C_{\rm rad} + g^L_{\rm rad}) \;=\; \frac{\sigma_{\rm eff}(r)}{c} \frac{L_*}{4\pi r^2} \;\; , \tag{2.101}$$

and use the velocity law (obtained via a previous iteration in the temperature structure) to solve for $\sigma_{\rm eff}$ as a function of radius from the equation of motion:

$$\frac{\sigma_{\rm eff}}{\sigma_e} = \frac{1}{,}\left[\left(1-\frac{1}{u^2}\right)w - H(x) + ,\right] \quad . \tag{2.102}$$

This scattering coefficient allows an optical depth variable to be defined,

$$\tilde{\tau} = \int_r^\infty \sigma_{\rm eff}\,\rho\left(\frac{R_*}{r}\right)^2 dr \quad , \tag{2.103}$$

which here assumes an isotropic Eddington factor $f_\nu \equiv K_\nu/J_\nu = 1/3$, as opposed to the radial-streaming value $f_\nu = 1$ assumed in eq. (2.100) above (see Mihalas 1978). This optical depth can be used in a modified Milne-Eddington temperature distribution for a spherically extended gray atmosphere in radiative equilibrium,

$$T(r)^4 = \frac{1}{2}T_{\rm eff}^4\left(2W + \frac{3}{2}\tilde{\tau}\right) \quad , \tag{2.104}$$

where the dilution factor W is given by eq. (2.87). In the optically-thin limit, $T(r)$ depends only on $W^{1/4}$, which varies very slowly with radius. This method of zero-order radiative transfer takes into account "line blanketing" due to the spectral lines that contributed to the line radiation force, but is necessarily limited by the many approximations discussed above.

2.3.2 Analytic Approximations and Empirical Fits

The first analytic solution of the Sobolev wind equations was that of CAK, who ignored the finite disk factor ($\eta = 1$), considered constant values of k and α with radius, and neglected the ionization factor δ. Also, since gas pressure forces play a relatively minor role in driving the highly-supersonic wind, one can neglect these terms ($a \to 0$) in the CAK wind equation (2.89). In fact, the assumption of "zero sound speed" is an approximation of the same order as the use of the Sobolev approximation in both the subsonic and supersonic regions. The wind equation becomes, in the limit $a \to 0$ (or, equivalently, $u \gg 1$),

$$F_1 \approx w + 1 - , \; - Cw^\alpha = 0 \quad , \tag{2.105}$$

and the singularity condition

$$F_2 = \frac{\partial F_1}{\partial w} \approx 1 - \alpha C w^{\alpha-1} = 0 \tag{2.106}$$

allows for the immediate solution of w and C at the critical point,

$$w_c = \frac{\alpha}{1-\alpha}(1 - , \;) \quad , \qquad C = \frac{1}{\alpha^\alpha}\left(\frac{1-,}{1-\alpha}\right)^{1-\alpha} \quad . \tag{2.107}$$

Note, however, that the equation $F_1 = 0$ here does not depend on the radius r. Thus, if one point in the wind satisfies the critical conditions, all points do, and $w \propto r^2 v(dv/dr)$ remains *constant* in the wind. Thus, one can immediately integrate from the stellar radius R_*, and obtain

$$v_{\rm CAK}(r) = v_\infty \left(1 - \frac{R_*}{r}\right)^{1/2} \quad , \tag{2.108}$$

where the asymptotic ("terminal") wind speed is given by

$$v_\infty = \sqrt{\frac{\alpha}{1-\alpha} \frac{2GM_*(1-,)}{R_*}} = \sqrt{\frac{\alpha}{1-\alpha}}\, V_{\rm esc} \quad . \tag{2.109}$$

In addition, the mass loss rate can be found from the definition of the constant C (and, of course, the assumption that k and α remain constant throughout the wind), and

$$\dot{M}_{\rm CAK} = \frac{L_*}{c^2} \left\{ \alpha k^{1/\alpha} \left(\frac{c}{v_{th}}\right) \left[\frac{(1-\alpha),}{1-,}\right]^{(1-\alpha)/\alpha} \right\} \quad . \tag{2.110}$$

For our standard model of ζ Puppis this CAK analysis yields $v_\infty = 1080$ km s^{-1} and $\dot{M} = 5.9 \times 10^{-6}\, M_\odot {\rm yr}^{-1}$, and the terminal velocity v_∞ is quite different from the observed value. The mass loss rate scales with $k^{1/\alpha}$, so modeling a given $\dot{M}$, at least in an *ad hoc* fashion, is not difficult. CAK also computed numerical models with finite gas pressure terms, and found only small variations from the analytic results above. However, these models allowed the computation of a unique critical radius x_c, which CAK found to be approximately 1.5–1.7 times the sonic radius x_s, which is the radius at which $v = a$, and is usually extremely close to the photosphere ($x_s \approx 1$).

The critical radius x_c and velocity u_c can be estimated by applying the regularity condition $F_3 = 0$ to the wind equation (2.91), with no finite disk factor ($\eta = 1$), but *retaining* the small terms proportional to the finite sound speed. Thus,

$$F_3 = \frac{\partial F_1}{\partial x} + \left(\frac{\Pi w}{u x^2}\right) \frac{\partial F_1}{\partial u} = -\frac{2}{\Pi} + \frac{2\Pi w^2}{u^4 x^2} = 0 \quad , \tag{2.111}$$

and we can solve for the critical radius

$$x_c = \frac{\Pi w_c}{u_c^2} \quad . \tag{2.112}$$

Because the addition of a finite sound speed only significantly affects the wind in the subsonic region, one can use the value of w_c derived above in the *zero* sound speed limit, and the associated velocity (evaluated at x_c),

$$u_c = \frac{v_\infty}{a} \sqrt{1 - \frac{1}{x_c}} \quad , \tag{2.113}$$

to find that the critical radius in this approximation is exactly 1.5 times the stellar radius:

$$x_c = 1 + \frac{\Pi w_c}{(v_\infty/a)^2} \;=\; 1 + \frac{1}{2} \;. \tag{2.114}$$

This comes very close to the actual values found by self-consistently integrating the differential equation $F_1 = 0$ and evaluating the optical depth (or velocity) at the stellar surface (CAK).

Strictly speaking, when finite sound speed terms are included in the CAK equation of motion, the velocity never reaches an asymptotic terminal velocity v_∞, and instead grows logarithmically without bound as $r \to \infty$. This occurs because of the sound speed term $2a^2/r$ which dominates the expansion exterior to the "Parker radius" ($R_P = GM_*/2a^2 \gg R_*$). More realistic models with a decreasing wind *temperature,* however, negate the importance of this term at large radii, and a reasonably constant terminal v_∞ is achieved.

Friend and Abbott (1986, hereafter FA), nearly simultaneously with PPK, extended CAK's theoretical framework by including the uniformly-bright *finite disk factor* (see Section 2.2.4), gas pressure terms, and rotation in the equatorial plane. Least squares fits to the numerical results of FA give a similar velocity law,

$$v_{\rm FA}(r) \;=\; v_\infty \left(1 - \frac{R_*}{r}\right)^\beta \;, \tag{2.115}$$

but with $\beta \approx 0.8$, and

$$v_\infty \;\approx\; 2.2\, V_{\rm esc}\, \frac{\alpha}{1-\alpha} \left(\frac{V_{\rm esc}}{10^3 \text{ km s}^{-1}}\right)^{0.2} \left(1 - \frac{V_{\rm eq}}{V_{\rm crit}}\right)^{0.35} \;, \tag{2.116}$$

$$\dot{M}_{\rm FA} \;\approx\; \frac{1}{2}\dot{M}_{\rm CAK} \left(\frac{V_{\rm esc}}{10^3 \text{ km s}^{-1}}\right)^{-0.3} \left(1 - \frac{V_{\rm eq}}{V_{\rm crit}}\right)^{-0.43} \;, \tag{2.117}$$

where the rotational dependence of $\dot{M}_{\rm FA}$ was obtained by Bjorkman and Cassinelli (1993) from FA's Figure 4 (see Chapter 4 for more information on rotating models). The inclusion of the finite disk factor decreases the radiation force near the base of the wind; i.e., $\eta \to 1/(1+\alpha)$ as $r \to R_*$, because there are comparatively fewer radially-directed photons near a source of large "horizontal" extent, but $\eta \to 1$ as $r \to \infty$, because the star looks more like a point source as one recedes from it. The mass loss rate, which is determined in the vicinity of the critical point, is thus reduced. Because less material is accelerated into the outer parts of the wind, where the force becomes close to the point-star force, the terminal velocity increases. The inclusion of the finite disk factor, then, causes roughly no change in the final wind momentum $\dot{M}v_\infty$, but their individual values agree much better

with the observations: for the same assumed α and k constants as above, FA's fit formulae give, for the standard nonrotating ζ Puppis model, $v_\infty = 2850$ km s^{-1} and $\dot{M} = 3.0 \times 10^{-6}\, M_\odot \mathrm{yr}^{-1}$.

In these models, the critical radius also becomes smaller, with $x_c \approx 1.02 - 1.05$, but moves outward with increasing rotation rate. Because x_c is so close to the stellar surface, Gayley, Owocki, & Cranmer (1995) found that it is reasonably safe to assume a constant critical value for the finite disk factor $\eta_c \equiv 1/(1+\alpha)$, and estimate the modified mass loss rate as if η_c were simply a constant multiplying k, i.e.,

$$\dot{M}_{\rm FD} \approx \eta_c^{1/\alpha} \dot{M}_{\rm CAK} \quad . \tag{2.118}$$

For the above model of ζ Puppis, this factor reduces the CAK mass loss rate to $2.7 \times 10^{-6}\, M_\odot \mathrm{yr}^{-1}$.

Note that while the mass loss rate is determined at the critical point, very close to the star, v_∞ is determined effectively at *infinite* radius (because it is "built up" cumulatively, once the mass flux is known that can be driven to infinity). Assuming that the radial velocity obeys a "beta law" at large radii,

$$v_r(r) = v_\infty \left(1 - \frac{R_*}{r}\right)^\beta \quad , \qquad \frac{\partial v_r}{\partial r} = \frac{\beta v_\infty R_*}{r^2} \left(1 - \frac{R_*}{r}\right)^{\beta-1} \quad , \tag{2.119}$$

we can substitute this back into the zero-sound speed equation of motion and take the limit $r \to \infty$. At large radii, we can ignore the finite disk factor (because the star appears as a point source) and write eq. (2.105) in this limit as

$$U^2 + 1 - , \ - C U^{2\alpha} = 0 \quad , \tag{2.120}$$

where $U \equiv (v_\infty / V_{\rm esc})(2\beta)^{1/2}$ and $V_{\rm esc} \equiv (2GM_*/R_*)^{1/2}$. Thus, if $\dot{M}$ is estimated as above, the above algebraic equation can be solved (numerically, if $\alpha \neq 0.5$) for U. The weak dependence in U on the unknown value of β is a minor disadvantage, but it only results in a 10–20% uncertainty in the final value of v_∞.

For α close to 0.5 we can Taylor-expand the slowly-varying function $U^{2\alpha}$ about a constant U_0:

$$U^{2\alpha} = U_0^{2\alpha} + 2\alpha\,(U - U_0)\,U_0^{2\alpha-1} + \cdots \tag{2.121}$$

$$\approx U_0^{2\alpha} \left[(1 - 2\alpha) + 2\alpha\,(U/U_0)\right] \quad . \tag{2.122}$$

If we take $U_0 = 1$,

$$U \approx \alpha C \pm \sqrt{\alpha^2 C^2 - 2\alpha C - 1 + , \ + C} \sim 2\alpha C \quad , \tag{2.123}$$

and the positive solution is the physically realistic one. Note, however, that the exact solution to the transcendental equation (2.120) is more accurate, and this

Taylor expansion is presented only to illustrate how U is approximately dependent on α and C in this analysis. However, eq. (2.123) does illustrate the fact that, for $\dot{M}$ too large, or C too small, there will be no steady state solutions driven to infinity. In fact, the minimum value of C (found by setting the terms under the square root to zero) is remarkably close (within $\sim 2\%$ for $\alpha = 0.5$–0.7) to the critical point-star value of C found above (eq. [2.107]). For the standard nonrotating ζ Puppis model, eq. (2.120) is solved by $v_\infty = 2688$ km s^{-1} (if we assume $\beta = 0.8$), and the above expansion yields $v_\infty \approx 2374$ km s^{-1}.

More recent sets of semi-analytic models have provided better, but more complex fitting formulae for v_∞, $\dot{M}$, and β of O and B stars. PPK computed grids of models taking into account the finite disk factor, gas pressure terms, and a line force dependent on the state of ionization of the wind. They fit closed-form scaling relations to v_∞ and $\dot{M}$, but the equations are too complex to be reproduced here. Of interest, however, is a fit for the exponent β for models with $T_{\rm eff}$ in the range 20000–50000 K,

$$\beta \approx 0.97\alpha + 0.032 \left(\frac{V_{\rm esc}}{500\,{\rm km\ s^{-1}}} \right) + \frac{0.008}{\delta} \quad , \tag{2.124}$$

where δ is the exponent in the line force modified to take varying stages of ionization into account (see Section 2.2.5). Kudritzki et al. (1989) and Villata (1992) have built up more complex, but more robust expressions for v_∞ and $\dot{M}$. The detailed finite disk and ionization correction factors are modeled approximately as functions of radius only, so that the implicit differential equation of motion can be solved "graphically" (i.e., with numerical root-finding techniques) as an algebraic equation in x, u, and w. Specifically, the Kudritzki et al. (1989) "cooking recipe" gives $v_\infty = 2649$ km s^{-1} and $\dot{M} = 3.8 \times 10^{-6}\, M_\odot {\rm yr}^{-1}$ for the standard ζ Puppis model star.

2.3.3 Numerical Wind Models

The one-dimensional CAK equation of motion (eq. [2.91]) can be solved numerically in several ways. Here we discuss two such solution methods: (1) the "modified CAK" (mCAK) approach, which iteratively locates the critical point and integrates upward and downward from it in radius, and (2) full time-dependent hydrodynamics (using the piecewise parabolic code VH-1) which evolves an approximate initial condition to find possible steady end-states.

The mCAK method first requires the critical values of x_c, u_c, w_c, and C to be found, as discussed above. By starting from an assumed critical radius x_c and, e.g., FA's empirical velocity law fit as an initial guess, we use the Newton-Raphson method of finding roots of the nonlinear system of equations $F_1 = F_2 = F_3 = 0$

to evaluate u_c, w_c, and C. The fact that the wind equation itself ($F_1 = 0$) can be algebraically solved for C allows us to collapse the nonlinear search space from three to two dimensions. After substituting this value of C into the singularity and regularity equations, the Newton-Raphson correction equation

$$\begin{pmatrix} \partial F_2/\partial u & \partial F_2/\partial w \\ \partial F_3/\partial u & \partial F_3/\partial w \end{pmatrix} \begin{pmatrix} \delta u \\ \delta w \end{pmatrix} = \begin{pmatrix} -F_2 \\ -F_3 \end{pmatrix} \tag{2.125}$$

is easily solved for the incremental corrections to u_c and w_c (δu and δw). Various "acceleration" techniques can be used to improve the convergence of this procedure, (see, e.g., Press et al. 1989), but a good starting guess is of primary importance to the rapid convergence of a solution.

With all dynamical variables determined at the critical point, one can integrate inwards and outwards by numerically solving eq. (2.91) for w, and thus du/dx, and stepping up and down in x with a numerical integration routine. In most of the wind, two solution branches for w exist, and the critical point is the place where the wind switches from one branch to the other. For $x < x_c$, the lower of the two values of w ($w < w_c$) is the correct solution, and for $x > x_c$, the higher of the two values of w ($w > w_c$) is the correct solution.

Figure 2.2 shows the resulting mCAK singular locus, critical point, and velocity law for the standard ζ Puppis model star, assuming a uniformly-bright finite disk factor. Only the near-star wind is shown to illustrate the grazing of the singular locus at the critical point. Also shown is the "quasi-static" exponential velocity law which is the limiting case for the deep subsonic wind ($v_r \ll a$). In this region, the radial momentum equation simplifies to the equation of hydrostatic equilibrium

$$\frac{\partial P}{\partial r} \;=\; -\rho\, g_{\rm eff} \;=\; -\rho\, \frac{GM_*(1-,)}{r^2} \quad , \tag{2.126}$$

which is solved for an isothermal medium by the exponentially decreasing density,

$$\rho(r) \;=\; \rho_0 \exp\left[-(r-R_*)/H_\rho\right] \quad , \tag{2.127}$$

where $H_\rho \equiv a^2/g_{\rm eff}$ is the density scale height. The subsonic radial velocity is thus given by the mass continuity equation, and

$$v_r(r) \;=\; \left(\frac{\dot{M}}{4\pi R_*^2 \rho_0}\right) \exp\left[+(r-R_*)/H_\rho\right] \quad . \tag{2.128}$$

Of course, as the wind accelerates past the sonic point, the density no longer drops exponentially, but approaches a $1/r^2$ power law as $v_r \to v_\infty$.

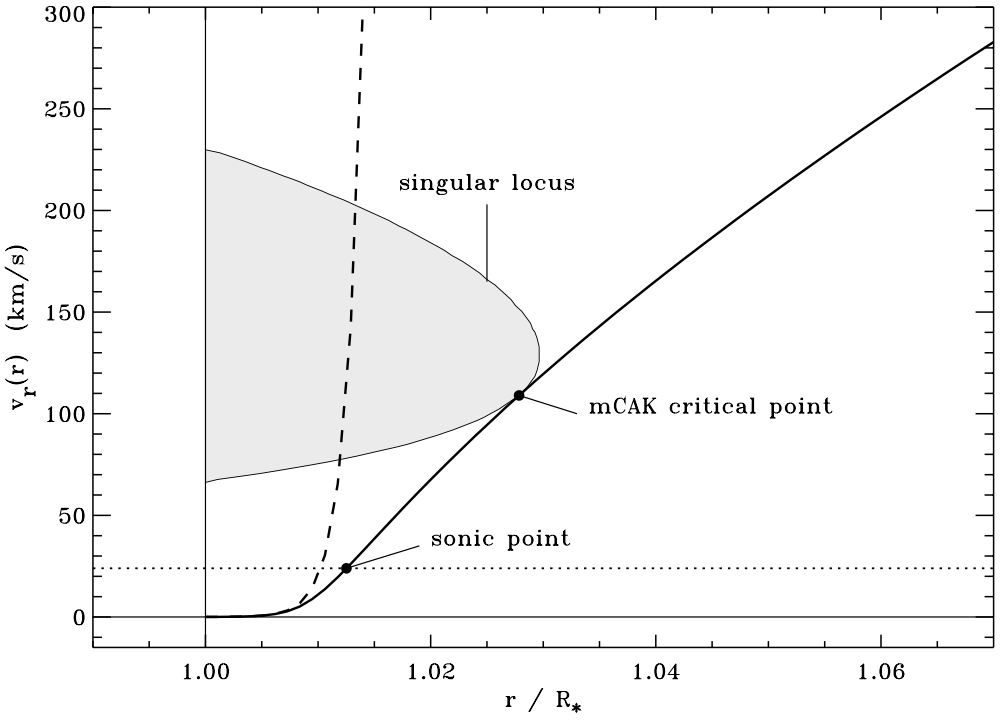

Figure 2.2: Solution topology for the mCAK model of ζ Puppis. The shaded region contains no solutions to the equation of motion, and is bounded by the singular locus of one solution. Also shown are the numerical velocity law (thick solid line), the subsonic exponential approximation for the velocity (dashed line), and the sound speed of the gas (dotted line).

Table 2.1 and Figure 2.3 illustrate the effect of varying the line-driving constants α, k, and δ on the resulting wind solutions. Note that varying k has absolutely no effect on the velocity law $v_r(r)$, but only on the mass loss rate $\dot{M}$. This can be seen in the zero sound speed solutions, and by the fact that the critical value of the constant C (which contains k and $\dot{M}$) itself depends only on α, , , and the assumed finite disk factor. Note also that, as far as the velocity law (v_∞ and $\beta_{\rm eff}$) is concerned, the exponent δ acts as a "negative α," and v_∞ and $\beta_{\rm eff}$ depend mainly on the quantity $\alpha - \delta$ (see Kudritzki et al. 1989). This trend does not extend to $\dot{M}$ and the location of the critical point x_c, however, because the N_{11}^{δ} factor in the radiative force is present in the definition of C as an effective "radially-dependent k."

The effective beta exponent $\beta_{\rm eff}$ listed in Table 2.1 and plotted in Figure 2.3 is defined using the parameterized velocity law (eq. [2.119]) as

$$\beta_{\rm eff}(r) \;=\; \left(\frac{r}{R_*} - 1\right) \frac{r}{v_r} \frac{\partial v_r}{\partial r} \quad , \tag{2.129}$$

and is a convenient measure of the wind's acceleration. We evaluate $\beta_{\rm eff}$ at $r = 2R_*$, which is a canonical median wind location, close to the points where $v_r \approx v_\infty/2$ and $\sigma = 0$ (isotropic expansion) in most wind models. At this point, $\beta_{\rm eff}$ is expressible as

$$\beta_{\rm eff} \;=\; \frac{\log[v_r(r = 2R_*)/v_\infty]}{\log(1/2)} \quad . \tag{2.130}$$

Next we apply a time-dependent numerical hydrodynamics code to the problem of a radiatively driven wind. By including time dependence (in the $\partial/\partial t$ terms previously ignored by the mCAK analysis) we introduce the possibility of finding variable or discontinuous solutions to the wind equations, and we also become able to assess the *stability* of steady-state solutions. The numerical code, VH-1, was developed by J. M. Blondin and colleagues at the University of Virginia, and uses the piecewise parabolic method (PPM) algorithm developed by Collela & Woodward (1984). VH-1 solves the Lagrangian forms of the equations of hydrodynamics in the fluid rest frame, and remaps conserved quantities onto an Eulerian grid at each time step.

In its most general form, VH-1 solves the three-dimensional equations of mass, momentum, and energy conservation (eqs. [2.1]–[2.3]) in an arbitrary coordinate system, but here we examine a one-dimensional spherically symmetric geometry. Also, in all models computed here the energy conservation is dominated by rapid radiative processes, which keep the gas very nearly isothermal with a constant wind temperature T equal to the stellar effective temperature $T_{\rm eff}$. We use a perfect gas law equation of state to evaluate the pressure P. The radiative force due to continuum and line processes is computed as in the mCAK method above, with

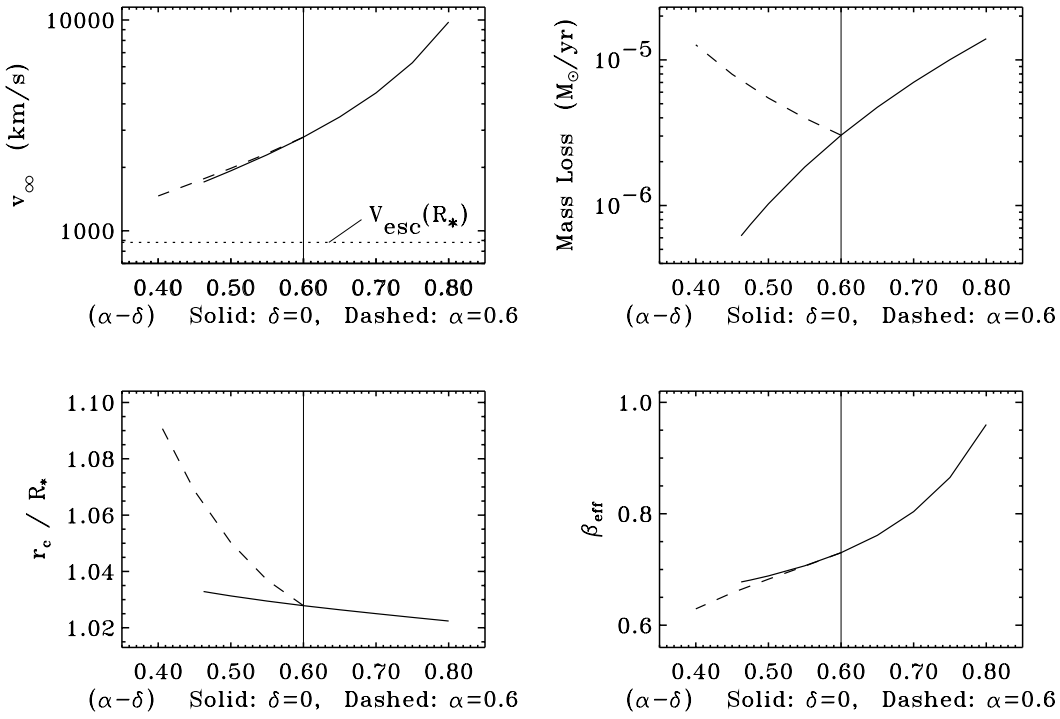

Figure 2.3: Parameter study for various mCAK wind models. Shown are the terminal velocity, mass loss rate, critical radius, and effective beta exponent. The solid line represents models with $\delta = 0$ (thus plotting α as the independent variable), and the dashed line represents models with $\alpha = 0.6$ (thus plotting $[0.6 - \delta]$ as the independent variable).

Table 2.1: Parameter Study for mCAK Standard Model

α	k	δ	v_∞ (km s^{-1})	$\dot{M}$ ($M_\odot$yr^{-1})	x_c	$\beta_{\rm eff}$
			Varying mCAK α			
0.4625	0.15	0.00	1702.74	6.19453 $\times 10^{-7}$	1.032877	0.67761
0.4750	0.15	0.00	1773.16	7.38506 $\times 10^{-7}$	1.032334	0.68101
0.5000	0.15	0.00	1926.19	1.02630 $\times 10^{-6}$	1.031311	0.68847
0.5500	0.15	0.00	2294.36	1.83761 $\times 10^{-6}$	1.029477	0.70658
0.6000	0.15	0.00	2782.85	3.03821 $\times 10^{-6}$	1.027855	0.73009
0.6500	0.15	0.00	3469.08	4.72661 $\times 10^{-6}$	1.026383	0.76123
0.7000	0.15	0.00	4509.55	7.01519 $\times 10^{-6}$	1.025009	0.80386
0.7500	0.15	0.00	6267.86	1.00384 $\times 10^{-5}$	1.023691	0.86517
0.8000	0.15	0.00	9780.13	1.39673 $\times 10^{-5}$	1.022387	0.96012
			Varying mCAK k			
0.6000	0.10	0.00	2782.85	1.54573 $\times 10^{-6}$	1.027855	0.73009
0.6000	0.15	0.00	2782.85	3.03821 $\times 10^{-6}$	1.027855	0.73009
0.6000	0.20	0.00	2782.85	4.90737 $\times 10^{-6}$	1.027855	0.73009
			Varying mCAK δ			
0.6000	0.15	0.00	2782.85	3.03821 $\times 10^{-6}$	1.027855	0.73009
0.6000	0.15	0.05	2328.37	3.98692 $\times 10^{-6}$	1.036940	0.70591
0.6000	0.15	0.10	1978.48	5.46630 $\times 10^{-6}$	1.050246	0.68255
0.6000	0.15	0.15	1698.05	7.96968 $\times 10^{-6}$	1.068636	0.65807
0.6000	0.15	0.20	1463.43	1.26802 $\times 10^{-5}$	1.093625	0.62929

the assumption of a uniformly-bright finite-disk factor and a power law ensemble of spectral lines defined by k, α, and δ.

We specify the boundary conditions in our numerical method in two phantom zones beyond each edge of the grid. At the outer radial boundary, the wind is invariably supersonic outward, and so we set the flow variables in the outer phantom zones by a simple constant-gradient extrapolation. The lower radial boundary of the wind is somewhat more problematic, and we use the boundary conditions described by Owocki et al. (1994): constant-slope extrapolation for v_r, rigid rotation for v_ϕ, and a fixed base density ρ_B. Because the mass loss rates of line-driven winds are determined from the equations of motion alone, we are able to specify an appropriate "photospheric" density that yields a stable, subsonic boundary outflow (see also Owocki, Castor, & Rybicki 1988). For our standard ζ Puppis model star, we choose a subsonic base density $\rho_B = 6 \times 10^{-11}$ g cm^{-3}, and we specify the flow variables on a fixed radial mesh with 200 zones, from R_* to $30R_*$. The zone spacing is concentrated near the stellar base where the flow gradients are largest; at the base, $\Delta r = 0.002R_*$ (which resolves the density scale height $H_\rho \approx [a/V_{\rm esc}]^2 R_*$), and it increases by 3% per zone out to a maximum of $\Delta r = 0.82R_*$ at the outer boundary.

This prescribed model has been implemented for various sets of stellar and wind parameters in this dissertation, and the hydrodynamics usually "settles" rapidly to a steady-state solution that agrees closely with the mCAK analysis. The models are stepped forward explicitly in time at a fixed fraction (0.25) of the Courant-Friedrichs-Lewy time step (see Press et al. 1989). The standard ζ Puppis star was modeled with VH-1, starting from an initial condition given by the mCAK velocity and density described above. The numerical wind solution relaxes to a steady state on a time scale comparable to the dynamical flow time for gas to radially advect across the computational grid,

$$t_d = \int_{r=R_*}^{30R_*} \frac{dr}{v_r(r)} \approx 2 \times 10^5 \, \mathrm{s} \quad . \tag{2.131}$$

Although a rigorous terminal velocity (at $r \to \infty$) cannot be computed for a model on a finite numerical grid, the dynamical variables at the outer radial grid zone are sufficient to compare with similar values from the mCAK analysis. The *ratio* of the VH-1 velocity and density to their corresponding mCAK values, for the ζ Puppis model at $30R_*$, are 1.0191 and 0.9515, respectively. Surprisingly, the major cause of these small differences at large radii probably is due to the slightly different treatments of the subsonic lower boundary.

2.4 An Overview of Non-Sobolev Wind Models

Although the Sobolev approach is used for all multidimensional and time dependent wind models in this dissertation, it is important to understand its limits, and under what circumstances a more rigorous model of the radiation driving becomes necessary. Also, the mCAK approximation of modeling the line ensemble using the (k, α, δ) distribution is another idealization that requires justification and scrutiny. Finally, the *stability* of the steady wind solutions to small perturbations is an important issue to resolve because the consequences of wind instability are potentially observable.

The primary research on extending the Sobolev and mCAK approximations has been undertaken by the Munich stellar astrophysics group in the 1980s and 1990s. PPK compared wind models using the Sobolev approximation to those constructed using a more accurate radiative force computed in the comoving frame of the flow, and found only negligible differences in the velocity laws and mass loss rates of the resulting winds. Even though the Sobolev approximation strongly underestimates the radiative force in the deeply subsonic wind ($v_r \lesssim v_{th}$) because it neglects diffuse radiation, the overall *magnitude* of the radiative force, compared to gas pressure and gravity, is small in this region. The mean end result, then, is insensitive to the force computed there.

The mCAK line ensemble approximation was relaxed by Pauldrach (1987), Pauldrach & Herrero (1988), and Pauldrach et al. (1990), who treated the full multilevel non-LTE problem for tens of thousands of line transitions, as well as a detailed continuum opacity containing bound-free and free-free opacity from dozens of elements. These models resulted in an improved comparison to observations of both the overall v_∞ and $\dot{M}$ values and the detailed profile shapes of individual lines. In most cases, however, the wind dynamics can be characterized well by simply modifying the k, α, and δ force constants in the mCAK model based on this improved radiative transfer. The existence of overlapping lines, and thus the presence of *multiple scattering* of photons, has been treated in both a statistical manner (Friend & Castor 1983; Gayley et al. 1995) and by using detailed line-list and Monte Carlo radiative-transfer computations (Abbott & Lucy 1985; Puls 1987; Lucy & Abbott 1993; Springmann 1994). Although the dynamical properties of winds can be strongly affected when multiple scattering is important (see, e.g., eq. [2.52]), under certain approximations this effect can be treated as a simple "force multiplier" akin to the finite disk factor (Gayley et al. 1995).

Despite the above complications in the radiative transfer, then, a suitably modified version of the Sobolev/mCAK approach seems well-suited to modeling at least the mean dynamical properties of winds around hot stars. However, it

has been suspected since the work of Milne (1926) that the radiative force arising from spectral line opacity may be highly unstable to small perturbations. Lucy & Solomon (1970) noted that because the wind is optically thick in the driving lines, the majority of the force comes from photons within a thermal speed of the blue edge of each line. If a given wind parcel is perturbed slightly to a higher velocity, the blue edge shifts to shorter wavelengths (in the star's frame), where it sees additional *unshadowed* photons which can further accelerate the parcel, thus blueshifting the line profile even more, and so on.

This instability was confirmed by MacGregor, Hartmann, & Raymond (1979) and Carlberg (1980), who performed linear perturbation analyses on the line force and assumed that the most important effect was the Doppler shift associated with the perturbed velocity. This work thus implicitly assumed that perturbations were optically thin, since associated velocity changes in the optical depth (eq. [2.26]) were neglected. However, a similar linearized analysis by Abbott (1980), which applied the Sobolev approximation to both the perturbation and the mean state, came to the opposite conclusion that line-driven winds are *stable* to small perturbations. In fact, Abbott (1980) found that such perturbations propagate as dispersionless "radiative-acoustic waves" at a phase speed which is a function of the mean mCAK-like force (see Chapter 7).

This apparent contradiction was resolved by Owocki & Rybicki (1984), who found that the instability depended sensitively on the length scale of the perturbation, and can be approximated by the "bridging law:"

$$\frac{\delta g_{\rm rad}}{g_{\rm rad,0}} \approx \frac{\delta v}{v_{th}} \left(\frac{ik}{2/L_{\rm Sob} + ik} \right) \quad , \tag{2.132}$$

where $\delta g_{\rm rad}$ is the first order force response to a velocity perturbation of the form $\delta v \propto \exp(ikr)$. In the limit of a large-scale perturbation ($k \ll 1/L_{\rm Sob}$), the Sobolev approximation is valid everywhere, and Abbott's (1980) marginally stable wave result of $\delta g_{\rm rad} \propto i\,\delta v$ applies. In the short-wavelength limit ($k \gg 1/L_{\rm Sob}$), the force and velocity perturbations are proportional, $\delta g_{\rm rad} \propto \delta v$, which is equivalent to the highly unstable optically-thin result of MacGregor et al. (1979) and Carlberg (1980).

Despite a great deal of subsequent research, this central conclusion of instability to small-scale perturbations remains. Lucy (1984) and Owocki & Rybicki (1985) investigated the effect of the *diffuse* radiation field on the instability, and found that it can be greatly reduced or even canceled near the stellar surface, but not in most of the supersonic wind. Rybicki, Owocki, & Castor (1990) extended this analysis into three dimensions and found that horizontal perturbations are more strongly damped than radial perturbations. Owocki & Zank (1991) discussed an effective "radiative viscosity" which arises from asymmetries in the diffuse radiation field, and how this

effect may help to suppress some of the intrinsic wind instability. Indeed, Gayley & Owocki (1995) found that for Wolf-Rayet winds, where the radiation is highly diffuse and photons multiply scatter, the growth rate of the instability is significantly smaller than for O and B stars (but still large enough for small perturbations to grow several orders of magnitude).

Owocki, Castor, & Rybicki (1988, hereafter OCR) performed the first *nonlinear* hydrodynamic calculations of unstable wind structure, and found that small perturbations rapidly grow into reverse shocks which separate high-speed rarefactions from slower, higher-density compressions. These models contained only the direct, pure-absorption radiative force, however. The effect of the scattered radiation field has been included by Owocki (1991, 1992) and Feldmeier (1995) via the "smooth source function" (SSF) approximation, which contains a nonlinear generalization of the Lucy (1984) line-drag and Owocki & Zank (1991) radiative viscosity effects. The SSF method does not compute the diffuse force arising from gradients in the perturbed source function, and Owocki & Puls (1996) have subsequently introduced the "escape integral source function" (EISF) method in order to better model the complex hydrodynamic phenomena which may result from these diffuse forces. The nonlinear structure in the supersonic wind, though, still appears to be dominated by stochastic reverse shocks, and the mean dynamical properties such as v_∞ and $\dot{M}$ appear to be relatively unaffected by the small-scale instability.